ABSTRACT

Adherent cells are able to actively generate internal forces, channelled by cytoskeletal protein filaments and transmitted through transmembrane receptors to the surrounding environment by means of focal adhesions. Cells also dynamically interact with extracellular matrix by sensing external chemo-mechanical stimuli and then inducing formation of stress fibres mediated by polymerization/de-polymerization processes which continuously redesign the interplay between structural organization and contractility activities in the cytoskeleton, so orchestrating selected signal pathways at the basis of many important cell's physiological functions like adhesion, migration and division. Despite chemo- and duro-taxis have been intensively studied in the last years to understand how cells move on a substrate, their polarization and reorientation – observed during gastrulation, wound healing and morphogenesis – are only partially understood. By starting from the evidence highlighted in some recent studies that cells reorient in response to substrata deformation by essentially obeying a pure mechanical interaction, we propose to interpret the seeming overall cells' rotation resulting from the reconfiguration of their cytoskeleton – here named *mechanotropism* – as a nonlinear optimization problem in which the adherent cell aims to align along directions leading it to minimize a physically coherent measure of work spent to deform the elastic substrate while retaining a prescribed level of homeostatic contractile force. To do this, the single-cell is simply modelled as a finite size contractile force dipole that acts on the boundary of a half-space perturbed by applied point loads. The effects of *fences* of forces acting orthogonally and tangentially on the boundary of the adhesion medium and encircling the cell are then investigated, so obtaining solutions that predict multiple non-trivial cell polarizations as functions of number, direction, relative magnitude and distance from the cell-dipole of the forces, as well as of the substrate's Poisson ratio, with unprecedented outcomes under the hypothesis of auxetic (i.e. negative Poisson ratio) materials. The results lead to envisage that the proposed theoretical model might contribute to unveil the mechanobiological principles ruling *in vivo* cells orientation processes by guiding the design of novel experimental strategies and to conceive new mechanics-based markers for guessing cells' pathological conditions from their mechanotropism.

1. Introduction

Along with biochemical factors, processes of mechanosensing and mechanotransduction play a pivotal role in regulating dominant aspects of cells' behaviour (Iskratsch et al., 2014; Mofrad and Kamm, 2009; Bao and Suresh, 2003; Banerjee et al., 2020; Fraldi and Carotenuto, 2018; Carotenuto et al., 2018, 2019).

As a matter of fact, necessary condition to the viability of the most cell lines (e.g. epithelial cells, fibroblasts, muscle cells) lies in their adhesion to a matrix able to offer an adequate stiffness to the continuous action of probing, by pushing and pulling, exerted by the single-cell via traction forces (Bershadsky et al., 2003; Harris et al., 1980). These are internally generated by a contractile

actomyosin cytoskeleton to maintain tissue homoeostasis and transmitted outwards through transcellular structures consisting of tension-dependent micrometre-sized aggregates of proteins (primarily integrins) known as focal adhesions (Ingber et al., 2014; Stamenović and Ingber, 2009; Deguchi et al., 2006; Riveline et al., 2001; Ferreira et al., 2020).

There are several evidences that, through focal adhesions' arrays, cells can recognize differences in the mechanical properties of the contact materials as well as sense the mechanical stimuli coming from the surrounding environment, namely forces and strains, and respond to them by altering their contractility level and structural organization, both locally (e.g. changes in stability and number of adhesion sites) and at a global scale, by remodelling the cytoskeletal machinery (Mofrad and Kamm, 2009; Geiger et al., 2009, 2001; Wang et al., 2009; Chen et al., 2015a; He et al., 2014; Brand et al., 2017; Loewe et al., 2020). As a consequence of the reaction to external mechanical perturbations, cell's physiological activities – including motility (Pelham and Wang, 1997; Lo et al., 2000), proliferation (Nelson et al., 2005) and differentiation (Engler et al., 2006) – are, in turn, re-modulated (Discher et al., 2005; Maul et al., 2011).

The physical and molecular principles that induce the cellular feedback under mechanical input and the way in which it actually realizes, thus moulding the cell behaviour, are however not yet fully understood. Therefore, uncovering of these mechanisms represents the cornerstone for the comprehension, the prediction and the potential control of critical biological phenomena developing both at the cell scale, such as phenotypic and neoplastic mutations, and at tissue level, in terms of morphogenesis, wound healing, remodelling and metastasis.

Within this framework, wide attention has been paid in the last years to the study of mechano-induced motility mechanisms of cells. For example, processes of mechanotaxis, namely of mechano-driven migration, have been detected, whose most consolidated evidence is represented by the stiffness-guided locomotion mechanism known as durotaxis (Lo et al., 2000; Lazopoulos and Stamenović, 2008). Additionally, (re)orientation and polarization of adherent cells have been largely recognized as influenced by their elastic interactions with the extracellular environment (Schwarz and Safran, 2013; He et al., 2020; Kopfer et al., 2020; Friedrich and Safran, 2012; Lim and Donahue, 2007). In this regard, it has been observed that animal cells, assuming round shapes in suspension, stretch and flatten when adhering to an external surface, some cell types (e.g. fibroblasts) assuming polarized (i.e. highly elongated) and stationary (i.e. non-migrating) profiles for sufficiently high values of the adhesion matrix rigidity (Prager-Khoutorsky et al., 2011; Lin et al., 2016). Laboratory outcomes have then highlighted that the orientation of these adherent cells does not arise randomly, rather it seems the result of an optimization process implemented by the cells for achieving some preferential conditions and maintain homoeostasis (Fraldi et al., 2019; De et al., 2008).

In particular, many works have shown that cells adhering to flat deformable substrates subject to pre-stretch or to static or cyclic stresses/stretches can rearrange from random to well defined angles through a sequence of disassemblies and reassemblies of the cytoskeletal apparatus, possibly combined with an actual rotation of the stress fibres (Deibler et al., 2011). Their final orientations depend both on the type of mechanical test (e.g. uni-axial or bi-axial loading) and on the frequency, duration and amplitude of the applied stretch/stress, some experiments also

evidencing threshold-activated behaviours in terms of frequency and/or magnitude (Wang et al., 1995, 2001; Tamiello et al., 2015; Xu et al., 2018). As an example, a rather common evidence is that, under uniaxial cyclic strains of the substrate, cells align nearly perpendicular to the loading direction at proper frequencies ($\sim$ 1 Hz), presumably in a way to avoid the perturbations arising from passive deformations and therefore to follow the direction of minimal substrate strain, a phenomenon designated as stretch avoidance (Jungbauer et al., 2008; Tamiello et al., 2015; Wang et al., 2001; Hayakawa et al., 2001). On the other hand, the cellular responses to static or quasi-static stretches are less understood (Schwarz and Safran, 2013), in this case cells having been found to principally arrange parallel to the stretching/force direction (Collinsworth et al., 2000; Xu et al., 2018; Eastwood et al., 1998; Steward et al., 2009; Liu et al., 2013), despite some other experiments have shown that they align randomly (Jungbauer et al., 2008) or that static stretch is not as influential as cyclic stretching in directing cell alignment and changing cell morphology (Goli-Malekabadi et al., 2011).

Motivated by these observations, a number of theoretical approaches have been proposed in the literature for studying the spatial organization and, in particular, the preferential alignments adopted by stationary single-cells as a consequence of the interplay with the network of neighbouring cells or the interaction with externally applied mechanical stimuli, often occurring through elastic media (Schwarz and Safran, 2013; Chen et al., 2015b). In this context, several possible optimization mechanisms have been suggested as underlying the reorientation process, each aimed to the achievement of a specific target, such as the attainment of the lowest strain state (Wang et al., 1995, 2001; De et al., 2008; Ben-Yaakov et al., 2015; Golkov and Shokef, 2017), the retention of a minimal or fixed stress level (De et al., 2007; Tondon and Kaunas, 2014; De et al., 2008; Ben-Yaakov et al., 2015; Golkov and Shokef, 2017), the search for the minimum elastic energy configuration (Schwarz and Safran, 2002; Bischofs and Schwarz, 2003; Livne et al., 2014; Xu et al., 2018) or the stability of the focal adhesions (Chen et al., 2012, 2015a; Fraldi et al., 2021). Accordingly, various mechanical descriptions have been provided, which range across different length scales, going from molecular approaches directly involving biochemo-mechanical processes at the level of the focal adhesion complexes to one- and bi-dimensional structural or continuum cellular models.

More in detail, widespread approaches predict that, under stretching of the substrate, cells realign along angles that allow them to maintain an optimal strain or stress state, namely along the zero or minimal strain directions (Wang et al., 1995, 2001; De et al., 2008; Ben-Yaakov et al., 2015; Golkov and Shokef, 2017) or in a way to retain a minimal or fixed (homeostatic) stress level (De et al., 2007; Tondon and Kaunas, 2014; De et al., 2008; Ben-Yaakov et al., 2015; Golkov and Shokef, 2017). As an example, among the models proposed in literature, De et al. (2007, 2008) studied stress fibres reorientation under both static and dynamic loading by supposing that cells tend to maintain an optimal (or set point) value of stress or strain in the adjacent matrix. In particular, motivated by experimental measurements of cellular traction patterns (Dembo and Wang, 1999; Schwarz et al., 2002), they used a coarse-grained modelling of the cells by approximating them as single anisotropic force dipoles (Schwarz and Safran, 2002).

On the other hand, different approaches involving macromolecular or biochemical descriptions of cellular orientation and stress fibres rearrangement in response to applied forces have also been discussed (Wei et al., 2008; Schwarz and Safran, 2013; Kaunas and Hsu, 2009; Hsu et al., 2009; Chen et al., 2012, 2015a; Kong et al., 2008). In this framework, Chen et al. (2012, 2015a) and Kong et al. (2008) for example proposed theoretical models based on the stability of the focal adhesions under cyclic loading. Recently, Xu et al. (2018) also developed a planar cytoskeletal tensegrity model, by incorporating the molecular mechanisms of focal adhesion dynamics, the actin polymerization and the actin retrograde flow, to study the dynamics of cell reorientation on a substrate under biaxial static and cyclic stretches.

Some other models have recognized in the search for a minimum elastic energy configuration the driving mechanisms for cell rearrangement (Livne et al., 2014; Schwarz and Safran, 2002; Bischofs and Schwarz, 2003). In particular, Livne and coworkers (Livne et al., 2014) developed a bi-dimensional model of the cell which takes into account both the passive elastic response of the cells to substrate deformation and the active remodelling of their actin cytoskeleton and focal adhesions, thus proposing that reorientation during cyclic stretching is driven by a dissipative process in which the passively stored elastic energy of the cell relaxes to a minimum through active realignment of the relevant molecular structures determining the final (optimal) orientation angle.

Finally, Safran and co-workers (Schwarz and Safran, 2002; Bischofs and Schwarz, 2003; Bischofs et al., 2004), by adopting a force dipole model for the adherent single-cell, analysed its interaction with the strain field induced on an elastic substrate homogeneously stretched along one axis under the assumption that cell positioning can be predicted by minimizing the interaction energy employed by the cell into straining its environment for a given level of force generation. The latter concepts were also used by the same authors to predict the collective response of contractile cells inside or over an elastic medium (Schwarz and Safran, 2002; Bischofs and Schwarz, 2003; Bischofs et al., 2004; Bischofs and Schwarz, 2005; Cohen and Safran, 2016), in order to investigate the preferred alignments of pairs or populations of elastically interacting cells in absence of externally applied loads and to highlight the influence of the substrate's elastic properties (specifically, of its Poisson ratio in case of isotropic material) on the coordinated multi-cellular orientation process (Bischofs and Schwarz, 2005).

In the present work, the mechano-induced orientation mechanism of adherent cells is named *mechanotropism*. A tropism (from the Greek word *τροπος*, tropos, ''a turning'') is a biological phenomenon indicating the turning movement (possibly accompanied by growth) of an organism, usually a plant, in response to an environmental stimulus. Phototropism, chemotropism and gravitropism are terms commonly adopted in biology for indicating the tendency of an organism to reorientate by responding to light, chemical and gravity stimuli, respectively. Accordingly, mechanotropism is here conceived as the process identifying the reorientation of a living system, in particular a cell, induced by mechanical stimuli, in this way also introducing a somehow complementary behaviour with respect to the cellular mechanotaxis.

By keeping in mind the results provided by the above-mentioned literature, we aim to propose a novel mechanical strategy that could help to uncover the optimization principles guiding the orientation process of cells elastically interacting with perturbing external forces through a

deformable substrate. With this purpose, the mechanotropism of an adherent single-cell is here theoretically studied under the effect of *ad hoc* conceived distributions of exogenous static loads, formed by point forces acting orthogonally and tangentially to the flat surface bounding the substrate of adhesion and located at the vertexes of a n-sided regular polygonal *fence* surrounding the cell.

Supported by both experimental measurements of cellular traction patterns and previous theoretical works (Schwarz et al., 2002; Schwarz and Safran, 2013, 2002; Bischofs et al., 2004), we model the polarized cell as a stretched one-dimensional fibre-shaped body acting as a pair of contractile forces at finite distance, i.e. a force dipole, on the boundary of a semi-infinite elastic isotropic and homogeneous solid, thus employing Boussinesq's and Cerruti's solutions to describe the mechanical interaction of the adherent cell with the fences of external point loads (Westergaard, 1952; Barber, 1992). In this regard, it is worth highlighting that, despite the concept of anisotropic force contraction dipole has been already used in the literature as paradigm for a dipolar-shaped cell (Schwarz and Safran, 2002, 2013), it has been treated by following a coarse-grained approach, namely by modelling the cell as a point defect in an elastic medium, thus assuming to observe it at a distance much larger than its spatial extent. Here, instead, in order to take also into account effects arising within areas proximal to the cell, we preserve the simplified physical picture of the force dipole but apply the two contractile forces by identifying the single-cell at two distinct point-sized sites of adhesion.

Cell's optimal orientations are then found by invoking as linchpin optimization principle the minimization of the magnitude of total work done by the cell to elastically deform the compliant substrate while retaining its traction forces level. By following this way, we find that the alignment of a cell is driven by its mechanotropism and hence decided by the interplay of few parameters describing the configurations of applied loads – forces' number n, direction, magnitude and distance from the cell – as well as by the Poisson ratio of the substrate, the latter leading to previously unseen results in case of auxetic (i.e. negative Poisson ratio) materials.

The work is organized as follows: Section 2 explains the main observations and assumptions on which the proposed strategy is grounded; Section 3 describes the theoretical model for the case of a cell-dipole elastically interacting with general distributions of exogenous point loads; Sections 4 and 5 specify the problem and discuss the results for the particular conditions of normal and tangent forces, respectively; Section 6 finally summarizes the aims and the contents of the work and opens to future perspectives.

2. Rationale and hypotheses underlying the theoretical model

Modelling of the single-cell as a force dipole on a semi-infinite substrate. It is known that stationary as well as migrating cells transmit traction forces to the substrate on which they lie through spatially localized focal adhesions complexes (Harris et al., 1980, 1981; Dembo and Wang, 1999). These in fact exhibit a strict correlation of their width and axis of elongation respectively with the magnitude and the direction of the force that they borne (Riveline et al., 2001; Balaban et al., 2001; Tan et al., 2003), such properties also resulting a function of the

stiffness of the underlying substrate (Pelham and Wang, 1997; Prager-Khoutorsky et al., 2011; Fusco et al., 2017; Ghibaudo et al., 2008).

In many cases (e.g. for suitable values of rigidity of the support material (Prager-Khoutorsky et al., 2011; Lin et al., 2016; Fusco et al., 2017)), stationary adhering cells, such as fibroblasts, assume highly elongated configurations (see Figs. 1A–B), characterized by focal adhesions principally located along the cell's rim and bearing significant forces only at the two extremities (Schwarz et al., 2002). These have magnitude of the order of 10–30 nN for each focal adhesion (corresponding to an average stress of about 5.5±2 nN/μm^2) and appear mainly oriented along the principal axis of the polarized cell, with a generally negligible projection along the direction orthogonal to the substrate surface (Balaban et al., 2001; Schwarz et al., 2002; Bershadsky et al., 2003; Ghibaudo et al., 2008). Moreover, the two tangent overall forces resulting, by superposition, at the opposite cell ends – actually directed along its polarization axis – appear to balance each other, in a way that, from the mechanical point of view, the whole adhering non-motile cell can be treated as a dipole of equal contractile forces, each of the order of hundreds of nN (Schwarz et al., 2002; Schwarz and Safran, 2002).

On the other hand, according to the constitutive and geometrical properties of the materials commonly used for plating cells during experimental tests and with the related observations about smallness of displacements and strains induced by the cell tractions with respect to the size of the substrate, it is reasonable to model the latter as an isotropic linear elastic semi-infinite solid, as in fact also commonly done in traction force microscopy techniques (Plotnikov et al., 2014; Balaban et al., 2001; Dembo and Wang, 1999; Schwarz et al., 2002; Schwarz and Safran, 2002; Sabass et al., 2008; Style et al., 2014).

On these bases, the effects of a polarized cell adhering on the top of an elastic substrate are here evaluated by employing for each of its two contractile forces the solution of the Cerruti's problem for tangent point load acting on the boundary of an half-space (see Appendix).

Elastic interaction with regular distributions of exogenous loads. It is assumed that the steadiness of a so-modelled stationary cell-dipole is perturbed by exogenous point loads acting, either orthogonally or tangentially, on the surface of the substrate as prescribed boundary conditions (see Fig. 1C). The influence of these forces is hence studied by coherently using superposed Boussinesq's or Cerruti's solutions (see Appendix), by prescribing different arrays of point loads, located at the vertexes of regular polygonal fences surrounding the cell, to gain insights into the mechanical principles driving the orientation of cell-dipoles by involving the minimum number of variable parameters to be also controlled in possible experimental tests.

It has to be noticed that, by considering a working temperature $\mathcal{T} = 310.15$ K and a scale length $a = 5$ nm corresponding to the diameter of the cytoskeletal protein filaments involved in the focal adhesion loci, rough calculations allow to estimate forces due to thermal fluctuations of the order of $k_B\mathcal{T}/a \simeq 10^{-13}$ N (k_B being the Boltzmann constant), well below the values of both cell traction forces and applied loads, which are greater than 10^{-7} N.

Stress homoeostasis via minimum deformation work as guiding principle for cell mechanotropism. Cells are systems continuously evolving to reorganize their cytoskeleton to respond to chemo-

mechanical stimuli. This implies that they are overall in a state of quasiequilibrium and that, during biological activities, they involve different forms of energy, both chemical (ATP) and of elastic (stored through pre-stress in stretched fibres) and entropic (e.g. due to head-tail interaction and unfolding of macromolecules) nature. However, these phenomena generally occur at different time-scales and elastic (mechanical) signals, as well as the electrical ones, travel significantly faster than others (Wang et al., 2009). A mechanical input can be hence considered immediately perceived by the cells as they transmit tractions to the elastic substrate and are in turn stimulated by reactive forces at the adhesion sites as well as when external forces are felt by cells via the elastic deformations induced on the substrate where they adhere. To respond to these perturbations and re-accommodate the structure in the best way for performing the physiological activities, cells tend to reorganize the cytoskeleton by means of combined processes of polymerization/depolymerization and internal repositioning of the protein filaments and of their arrangement, by doing work and spending energy.

In the case at hand, we assume that this structural reorganization, which overall can be seen as a re-orientation (mechanotropism) of the cell, is somehow decided by the cell itself to attain a state that can generate endogenous forces on the substrate (in vivo it is the extracellular matrix) aimed to determine cell homeostasis to be transferred across multiple length-scales up to the tissue level. In this sense, the proposed model is built up to make the single-cell capable to optimize its orientation in presence of external loads to retain an endogenous stress level as close as to the homeostatic one while minimizing the magnitude of work sensed in deforming the underlying substrate via the traction forces. This work comprises both a *self* energy spent by the cell-dipole due to its own action on the deformable substrate and an *interaction* energy due to the perturbation by the exogenous point forces (Bischofs and Schwarz, 2003), the latter being equivalent to the sole contribution often minimized in previous approaches under different kinds of boundary conditions (Bischofs et al., 2004).

Our assumption can be read as an application of the standard physical principle of energy (hence work as energy transfer) minimization and is supported by the observation that cells need to preserve and exploit their stored chemo-mechanical energy to fulfil their own physiological activities, as it also happens in well-established evidences of durotaxis (Lo et al., 2000). In that case, in fact, cell migration occurs towards directions of greater stiffness, which require lower work to maintain homeostatic levels of traction forces (Bischofs and Schwarz, 2003; Schwarz and Safran, 2013).

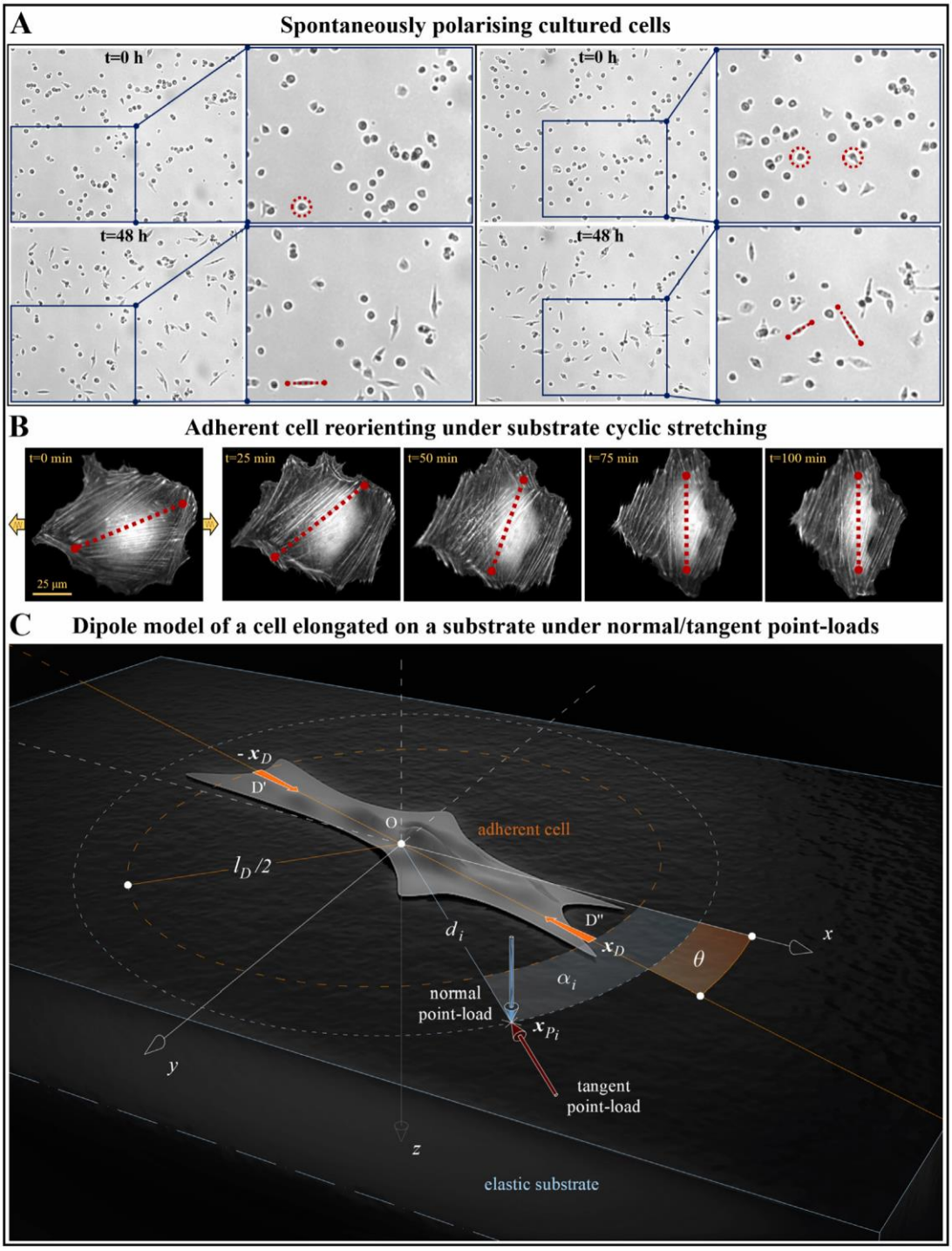

Fig. 1. (**A**) In vitro eukaryotic cells (normal adult prostatic epithelial cell PNT1A-ECACC 95012614) observed at optical microscope at different stages (0 and 48 h) with a zoom highlighting how they start from rounded shapes (red circles) to then orient and align in a preferred direction by forming stress fibres visualized as a force dipole (red lines with dots at the endpoints). Snapshots were obtained by the authors. (**B**) Example of the reorientation and elongation process

of a cell adhering to a substrate subjected to cyclic uniaxial stretching (8%,1 Hz): the tensed stress fibres and the whole cell body reconfigure by aligning quite perpendicularly to the direction of the applied stretch. The frames were captured and adapted from the video provided as supplementary material of the work by Deibler et al. (2011). (**C**) Three-dimensional sketch of an adherent stationary cell as a dipole of contractile forces acting tangentially on the top of the elastic substrate, under the action of exogenous forces in the form of normal and tangent point loads. The Cartesian reference frame as well as all the symbols and notations illustrated for denoting forces, angles and distances are the same as described throughout the main text.

3. Architecture of the model: *self* and *interaction* energies

On the basis of what highlighted above, a stationary adherent single-cell is here modelled as a dipole of contractile tangent forces having equal and constant magnitude and acting at a finite distance on the boundary of a homogeneous and isotropic linear elastic substrate.

In detail, as sketched in Fig. 1C, the cellular dipole is envisaged to be centred at the origin of the Cartesian reference system $\{x,y,z\}$, of unit vectors $\mathbf{e}_j$ with $j = x,y,z$, so that its two contractile forces can be written as

$$\mathbf{D}' = \mathbf{D} \text{ at } \mathbf{x} = -\mathbf{x}_D \text{ and } \mathbf{D}'' = -\mathbf{D} \text{ at } \mathbf{x} = \mathbf{x}_D \tag{3.1}$$

with

$$\mathbf{D} = \cos\theta\,\mathbf{e}_x + \sin\theta\,\mathbf{e}_y\, D \text{ and } \mathbf{x}_D = \cos\theta\,\mathbf{e}_x + \sin\theta\,\mathbf{e}_y\, l_D/2, \tag{3.2}$$

herein D indicating the magnitude of the dipole forces, l_D the dipole's length and, finally, the angle θ its (clockwise) orientation with respect to the x-axis that will be then used as cell's optimization parameter.

The generic external point load perturbation $\mathbf{P}_i$, applied at the point $\mathbf{x}_{Pi}$ of the semi-infinite substrate's boundary, can be given as

$$\mathbf{P}_i = P_i[\sin\phi_i\cos\gamma_i\,\mathbf{e}_x + \sin\phi_i\sin\gamma_i\,\mathbf{e}_y + \cos\phi_i\,\mathbf{e}_z],$$
$$\mathbf{x}_{Pi} = d_i\cos\alpha_i\,\mathbf{e}_x + \sin\alpha_i\,\mathbf{e}_y,\ i \in \{1,\ldots,n\}, \tag{3.3}$$

where n is the number of external perturbations, ϕ_i and γ_i represent the inclinations that the force $\mathbf{P}_i$ describes with the z-axis and the x-axis, respectively, P_i is the ith force's magnitude, while α_i is the angle that the position vector $\mathbf{x}_{Pi}$ forms with the x-axis and d_i the related distance from the axes origin.

The energy W that the cellular force dipole spends to deform the substrate in presence of a system of externally applied point loads can be written as the sum of two contributions, that is a *self* -energy W_D and an *interaction* energy W_{int}:

$$W = W_D + W_{int}. \tag{3.4}$$

Specifically, W_{int} identifies the amount of work that the cell traction forces perform through the displacements produced by the external perturbations. Hence, by virtue of the Betti's theorem, which finds the equality of the mutual works done by two systems of forces applied on a continuous linearly elastic body (Timoshenko and Goodier, 1967), it reads as

$$W_{int} = \mathbf{D} \cdot \mathbf{u}_{P_i} - \mathbf{x}_D - \mathbf{u}_{P_i} \mathbf{x}_D = \sum_{i=1}^{n} [\quad (\quad) \quad (\quad)] = \sum_{i=1}^{n} [\quad (\quad) \quad (\quad)] = \mathbf{P}_i \cdot \mathbf{u}_{D'} \mathbf{x}_{P_i} + \mathbf{u}_{D''} \mathbf{x}_{P_i} \quad , \tag{3.5}$$

( ) ( )

where $\mathbf{u}_{P_i} \pm \mathbf{x}_D$ are the displacements due to the force $\mathbf{P}_i$ at the extremities of the cellular dipole and, *vice versa*, $\mathbf{u}_{D'} \mathbf{x}_{P_i}$ and

$\mathbf{u}_{D''} \mathbf{x}_{P_i}$ are the ones induced by the cell forces $\mathbf{D}'$ and $\mathbf{D}''$, respectively, at the point of application of the ith perturbation. Note that, with reference to the first expression of W_{int} in (3.5), the sole in-plane displacement components produced by the external perturbations contribute to the interaction energy, since it is assumed that the cellular tractions have negligible normal component (Schwarz et al., 2002).

On the other hand, W_D indicates the quota of work that the cell does *per se* to deform the underlying medium while building up its own traction forces, regardless of the action of exogenous forces, so that

$$W_D = \frac{1}{2} [\quad (\quad) \quad (\quad) \quad (\quad) \quad (\quad)] \quad [\quad (\quad) \quad (\quad)] = \mathbf{D} \cdot \mathbf{u}_{D'} - \mathbf{x}_D - \mathbf{u}_{D'} \mathbf{x}_D + \mathbf{u}_{D''} - \mathbf{x}_D - \mathbf{u}_{D''} \mathbf{x}_D = \mathbf{D} \cdot \mathbf{u}_{D'} - \mathbf{x}_D + \mathbf{u}_{D''} - \mathbf{x}_D \quad , \tag{3.6}$$

() ( ) ′ and $\mathbf{D}''$, respectively, at the two points of adhesion of the cell where $\mathbf{u}_{D'} \pm \mathbf{x}_D$ and $\mathbf{u}_{D''} \pm \mathbf{x}_D$ are the displacements produced by $\mathbf{D}$

according to the solution of the Cerruti's problem — explicitly reported in Eq. (A.8) of Appendix. By virtue of the antisymmetrical arrangement of the dipolar forces with respect to the selected reference system and of the substrate material homogeneity, one has

( ) ( ) ( )

$\mathbf{u}_{D''} \pm \mathbf{x}_D = -\mathbf{u}_{D'} \mp \mathbf{x}_D$, whence the last equality in the equation above. Then, by taking into account

the divergence of the displacement field produced by a point load at its own site of application, the displacement $\mathbf{u}_{D'} - \mathbf{x}_D$ is here evaluated as arithmetic average of the displacements taken at two points placed at a distance r^{max}_C from the action point $-\mathbf{x}_D$ of the cell force $\mathbf{D}'$ along the direction θ of the dipole, say:

$$\mathbf{u}_{D'} - \mathbf{x}_D := \frac{1}{2} [\quad (\quad \overline{\quad} \quad max\hat{} D) + \mathbf{u}_{D'} (-\mathbf{x}_D + r_C max \mathbf{x}\hat{} D)] = \pi\mu\Sigma_{DD} \mathbf{x}\hat{} D, \tag{3.7}$$

$$- \mathbf{x}_D - r_C \mathbf{x} \quad 2$$

the second equality resulting from the Cerruti's solution (A.8) particularized for the case at hand. Therein, the hat denotes unit vectors and $\mu = E/2(1+\nu)$ is the shear modulus of the substrate, with E its Young modulus and ν the Poisson ratio. More specifically, $r^{max}_C \approx l_D/10$ represents an upper bound for the radius of the region in which the Cerruti's solution loses kinematical compatibility, evaluated for the case of a cell-dipole by considering the average values found in literature for the traction forces exerted by cells at focal adhesions' sites, for the length exhibited by polarized cells and for the stiffness of the substrates commonly used for experimental tests (see Appendix for details).

( )

The Cerruti's solution (A.8) can be finally applied to calculate $\mathbf{u}_D'' - \mathbf{x}_D$,[1] i.e.

$$\mathbf{u}_D''(\mathbf{x}_D) = -\frac{D}{2\pi\mu l_D^2}\left(\frac{2\nu-1}{2}\cos\theta\,\hat{\mathbf{e}}_x + \sin\theta\,\hat{\mathbf{e}}_x + \frac{2\nu-1}{2}\hat{\mathbf{e}}_z\right), \tag{3.8}$$

so that, by introducing expressions (3.7) and (3.8) into Eq. (3.6), the cell self-energy W_D reads as

$$W_D = \frac{9D^2}{2\pi\mu l_D}, \tag{3.9}$$

which – as expected due to the isotropy of the substrate material – does not depend on the particular orientation of the dipole. On the contrary, this evidently does not happen for the complementary contribute related to the interaction energy, whose explicit expression, deriving from Eq. (3.5), depends on the selected pattern of applied perturbations and is, in general, a function of the angle θ.

In this regard, by assuming that the sole degree of freedom for the considered stationary cell-dipole is represented by a rotational reconfiguration, we suppose, as motivated in the section above, that it orients along an optimal direction, identified by the angle θ, allowing it to minimize the intensity of the work W spent to deform the underlying substrate.

As a matter of fact, depending on the specific attributes of the external perturbation system (e.g. number and direction of point loads, ratio between their magnitude and that of the cell traction forces, distance from the cell centre, etc.), there could exist either configurations in which the cell-dipole is able to arrange itself in order to exactly nullify the total energy$\equiv W$ by exploiting advantageous orientations leading to obtain $W_{int} - W_D$ or, on the contrary, configurations such that, although not being able to wholly cancel W, the dipole orients in a way to minimize its absolute value, by properly modulating – through θ – the interaction contribute. This means that, in general, optimal orientations would be given by the angular points of the function $|W|$, represented by

$$\tilde{\theta}: W|\tilde{\theta} = 0, \tag{3.10}$$

under certain external conditions and, in complementary cases, by the stationary points

$$\tilde{\theta}: \partial_{\theta} W(\tilde{\theta}) = 0, \partial^2_{\theta} W(\tilde{\theta}) > 0. \tag{3.11}$$

In what follows, the effects induced on cell's orientation by selected patterns of forces acting either orthogonally or tangentially on the substrate boundary are studied.

4. Cell mechanotropism guided by fences of normal forces

Let us consider a fence of n point loads having equal magnitude and acting normally to the plane boundary of the semiinfinite deformable substrate at the vertexes of a regular (n-sided) polygon centred at the origin of the reference system $\{x,y,z\}$, which coincides with the midpoint of the cell-dipole. In such a case, the expressions in (3.3), defining the form of the generic ith perturbation, can be particularized by assuming $P_i = P$, $d_i = d$ and $\alpha_i = (i-1)2\pi/n$, $\forall i \in \{1,\dots,n\}$, and $\phi_i = 0$ for i indicating a downward-pointing force (i.e. a compressive force pointing towards the interior of the elastic half-space), while $\phi_i = \pi$ for i indicating a upward-pointing force (i.e. a tensile force), since the z-axis is directed downwards. This hence allows to write:

$$\mathbf{P}_i = \pm P \hat{\mathbf{e}}_z, \mathbf{x}_{Pi} = d\left\{\cos\left[(i-1)\frac{2\pi}{n}\right]\hat{\mathbf{e}}_x + \sin\left[(i-1)\frac{2\pi}{n}\right]\hat{\mathbf{e}}_y\right\}, \tag{4.1}$$

with plus and minus in $(4.1)_1$ identifying downward-pointing (compressive) and upward-pointing (tensile) forces, respectively. For sake of clarity, from now on, signs – and hence pointing directions – will be taken into account by adopting the following notation:
$P_d := +P$ and $P_u := -P$, where the subscripts "d" and "u" stand for downward and upward, respectively.

4.1. Cells encircled by a palisade of concordant point loads

By employing the Boussinesq's solution (reported in Eq. (A.5) of the Appendix) for each one of the n normal point loads here considered and by invoking the superposition principle, in the case in which such loads are either all downward-pointing or all upward-pointing, it is found that the interaction energy (3.5) can be expressed in the following general form

$$W_{int} = \frac{DP_{d,u}(1+\nu)(1-2\nu)m 2^{2-m/n}\left[1-\eta^m\cos(m\theta)\right]}{\pi E l_D \left[1+\eta^{2m}-2\eta^m\cos(m\theta)\right]}, \quad m = \begin{cases} n & n \text{ even} \\ 2n & n \text{ odd}, \end{cases} \tag{4.2}$$

---

[1] Upon calculation of the displacements $\mathbf{u}_{D'}(-\mathbf{x}_D)$ and $\mathbf{u}_{D''}(-\mathbf{x}_D)$, it is also possible to estimate the magnitude of the deformation (contraction) ε_D that the cell undergoes due to each of the two forces transmitted to the substrate. This is in fact given by:

$$\varepsilon_D = 1 - \frac{\| \mathbf{x}_D + \mathbf{u}_{D'}(\mathbf{x}_D) - (-\mathbf{x}_D + \mathbf{u}_{D'}(-\mathbf{x}_D)) \|}{l_D} = 1 - \frac{\| 2\mathbf{x}_D - (\mathbf{u}_{D'}(-\mathbf{x}_D) + \mathbf{u}_{D''}(-\mathbf{x}_D)) \|}{l_D}$$

$$= 1 - \frac{\sqrt{\left(4\left(2\pi\mu l_D^2 - 9D^2\right)^2 + (1-2\nu)^2 D^2\right)}}{4\pi\mu l_D^2},$$

which, by considering a limit case of high cell traction force and low substrate stiffness, namely $D = 1\,\mu\text{N}$ and $E = 10$ kPa, assumes values from 0 to ~ 0.12 for ν respectively varying from -1 (auxetic material (Lakes, 1987)) to $1/2$ (incompressible material), with $l_D \approx 50$-60 μm. This actually corroborates the assumption of working in a linear deformation regime in which small changes of the dipole's length – and thus approximately constant cell tractions – can be considered.

where the parameter $\eta := 2d/l_D$ is introduced. Note that the assumption $\eta > 1$ is here embraced, this meaning that any perturbation acts beyond the circular domain that the cell could potentially span during its orientation process.

By adopting expressions in (3.9) and (4.2) for the energy amounts W_D and W_{int}, respectively, the total work magnitude $|W|$ is minimum at its angular points

$$\tilde{\theta} = \pm \arccos\left(\frac{\left[\left(\eta^m - 9\cdot 2^{1+m/n} D + 4m(1-2\nu)Pd,u\right)\right]}{\eta^m}\right) + 2k\pi, \quad k \in \mathbb{Z}, \tag{4.3}$$

within ranges of the perturbations' parameters η and P such that:

$$1 \quad 9\cdot 2^{m/n} 1 + \eta^{2m} D + 4m(1-2\nu)P^{d,u}$$

$$\leq \quad 1 \quad \eta \leq \eta_c := \left|1 + 2\frac{}{2^{-m/n} m(1-2\nu)Pd,u}\right|^{1/m}, \quad \forall P_d \text{ and } P_u$$

$$< -9 \frac{}{}^{2} - 1 + m/n\, D, \tag{4.4}$$

$$9D$$

or, otherwise, at the following stationary points:

$$\tilde{\theta} = \begin{cases} 2k\pi \\ \left|\frac{}{(1+2k)\pi}\right|^{m/n}, \\ \left(\quad\right)^{1/m} \end{cases} \quad k \in \mathbb{Z}. \tag{4.5}$$

$$\text{when } \mathbf{P}_i = P_d \hat{\mathbf{e}}_z \,\forall i$$

$$\text{when } \mathbf{P}_i = P_u \hat{\mathbf{e}}_z \,\forall i$$

As a matter of fact, the solution is never influenced by the stiffness of the substrate but it rather depends on the number and the pointing direction of the normal perturbations. Additionally, the substrate's Poisson ratio, the relative magnitude of the applied loads with respect to the cellular force and, finally, the ratio η between the radius of the polygonal fence and the dipole (semi)length turn out to drive or not the cell orientation depending on whether this is provided by the null solution in (4.3) or by the stationary one in (4.5), respectively. In particular, since the stiffness does not contribute to determine the cell's alignment, the Poisson ratio is the sole elastic parameter

playing a role in cellular mechanotropism processes, at least when force-prescribed boundary conditions are considered[2].

By way of example, Fig. 2 shows the variation of the intensity of the elastic energy spent by a dipolar cell to deform the substrate in presence of a single external point load as function of its orientation angle θ.[3] By increasing η, for selected properties of the substrate and relative magnitude of the perturbation with respect to the cell force, one actually switches from a condition $\eta < \eta_c$ in which $|\mathcal{W}|$ owns a null point corresponding to its minimum (e.g. points **A1** and **B1**) to a status $\eta > \eta_c$ in which the minimum value is reached at a (non-zero) stationary point (as for points **A3** and **B3**), by passing through the limit situation $\eta = \eta_c$ where the null solution coincides with a stationary one (points **A2** and **B2**).

In the same figure, the optimal cell orientation $\tilde{\theta}$ is plotted as function of the relative distance parameter η, the shift from the solution in (4.3) to the one in (4.5) being therein evident (see points **A2** and **B2**). In particular, in this simple situation of single point load, the stationary solution (4.5) reduces to $\tilde{\theta} = 0$ for downward-pointing force and to $\tilde{\theta} = \pi/2$ for upward-pointing one: this means that, during a possible experimental study, one should observe in the former case an elongated cell arranged along a direction that contains the action point of the applied perturbation and in a way that such point lies in the direction orthogonal to the dipole's one, in the latter condition.

For a generic number n of concordant loads influencing the cell-dipole orientation and for every Poisson ratio of the substrate, the bounds in Eq. (4.4) allow to construct a chart in the P/D–η plane where one can identify domains in which the optimal configurations are provided by the solution in (4.3) nullifying the deformation work $\mathcal{W}$, and out of which the dipole arranges in accordance to the stationary points of $|\mathcal{W}|$ given in (4.5). Fig. 3 illustrates an example of such domains for both upward- and downward-pointing externally applied forces,[4] which one could helpfully consult for planning eventual experimental parameters and for predicting the optimal orientations that should be accordingly observed in cells. For instance, for both the possible pointing directions of the normal perturbations, two pairs of parameters P/D and η have been therein selected, that are $P/D = 70$ with $\eta = 1.4$ and $P/D = 10$ with $\eta = 1.8$, with the aim to respectively identify, for each considered n, a situation lying within the region $\eta < \eta_c$ and a complementary one, thus showing the optimal configurations that the cell could assume in each case. In this regard, it is worth noting that, in principle, the dipole could indifferently align along multiple optimal directions by undergoing the same energy expense. However, this reasonably occurs since no dissipative effects are associated to the cell orientation process in the presented model and, as a

---

[2] Actually, in the case of homogeneous and isotropic substrate, the reason why the Young modulus E is not involved in determining cell's orientation is that, in the formulation of the optimization problem, a term proportional to $1/E$ appears as a factor in the expression of the total work $\mathcal{W}$, so that it does not influence neither the null points of the latter nor the stationary points of its magnitude, differently from the Poisson ratio. However, this effect is likely related to the fact that the whole problem is studied by prescribing on the substrate boundary conditions that

involve only forces — the ones endogenously generated by the cell and transferred to the substrate and those applied as exogenous point loads. As a consequence, mixed or displacement-prescribed boundary conditions could be possible sources of a different sensitivity of the optimization (cell orientation) problem to the Young modulus. 3 It is worth to note that, in general, the minimum significant domain for the variable θ (and thus for the solution $\tilde{\theta}$) can be restricted to the range of values

$]\quad\ ]$

$-\pi/2,\pi/2$, since orientations out of such range describe equivalent configurations, due to the symmetry of the dipole. Also, note that graphics in Fig. 2 are

$[\ ]\tilde{}$, due to both the even character of the function $|W|$ when a single displayed by considering the restricted interval $0,\pi/2$ as reference domain for θ and θ orthogonal perturbation is applied at a point of the x-axis and the symmetry of the solution with respect to such axis in this case.

[4] As pointed out by Eq. (4.4), while the dipole can experience the possibility to nullify W for any ratio P/D under downward perturbations, on the contrary, it is necessary to apply upward forces with magnitude adequately higher than the cell's one to achieve the same result. For upward perturbations, Fig. 3 shows indeed a gap of values P/D for which the condition $\eta < \eta_c$ is never verified, whose width, by virtue of the last restriction about P_u in (4.4), is given by

$9 \cdot 2^{-1+m/\eta}[m(1-2\nu)]$.

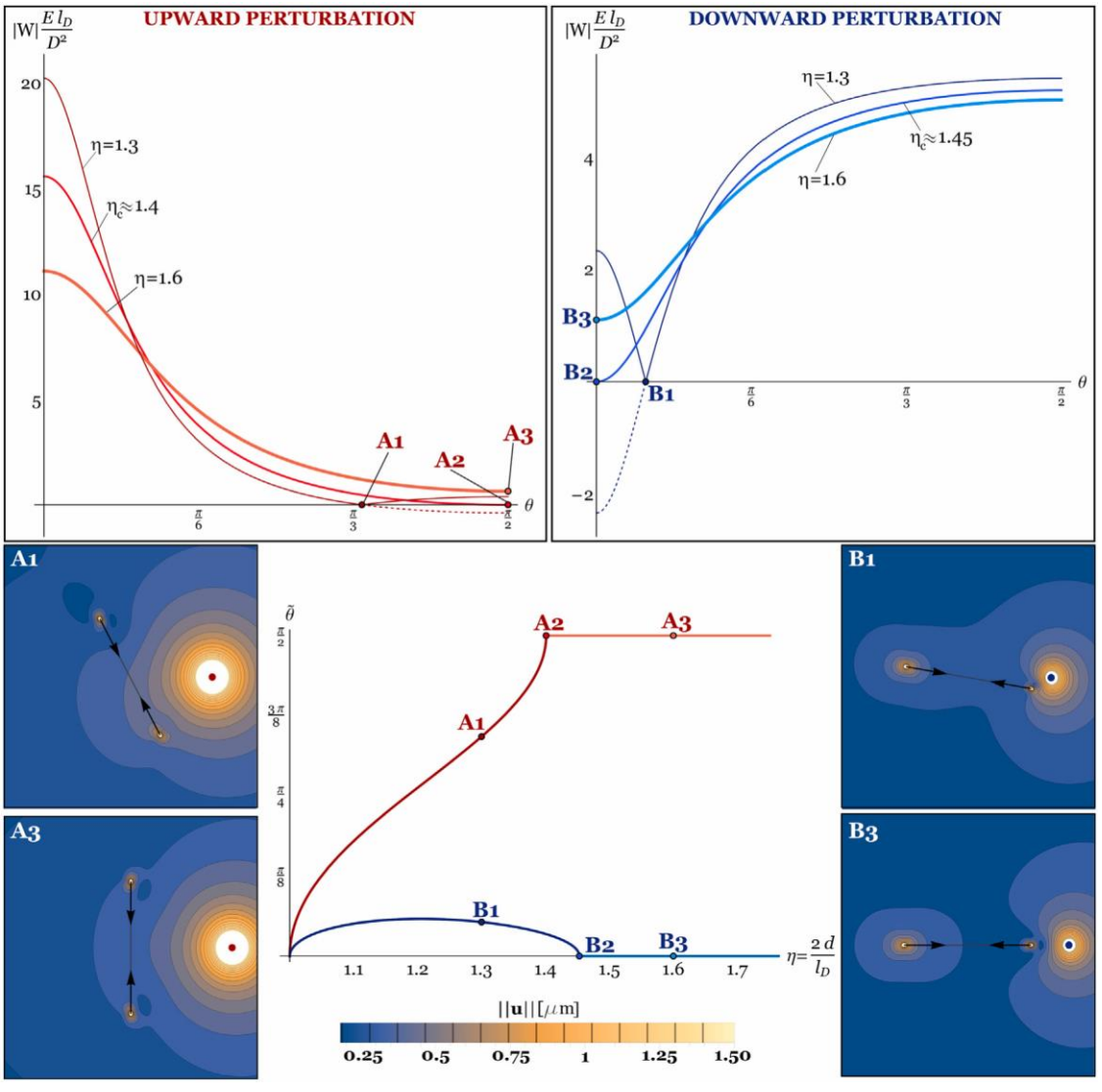

Fig. 2. At the top, the normalized absolute value of the elastic energy spent by the cell-dipole to deform the substrate of adhesion, plotted against the orientation θ

[ ]

varying within the range $0,\pi 2$, for both the cases of upward-pointing (left) and downward-pointing (right) single perturbation. The curves have been obtained by setting $\mathcal{P} = 40\mathcal{D}$ for the former case while $\mathcal{P} = 15\mathcal{D}$ for the latter one, with $\nu = 1/3$. Moreover, different values of the distance parameter η have been considered in order to cover all the conditions $\eta \lessgtr \eta_c$ analysed in the text. At the bottom, the solution $\tilde{\theta}$, that minimizes the deformation energy $|\mathcal{W}|$ when a single perturbation acts, is illustrated as function of η, through the red curve for upward-pointing load and the blue one for the complementary case. At the sides of such plot, there are focuses (top views) on the particular minimum energy configurations adopted by the cell-dipole (sketched as a couple of converging black arrows) at points **A1** and **B1** for which $\eta = 1.3 < \eta_c$ and points **A3** and **B3** characterized by $\eta = 1.6 > \eta_c$. On the background, there are contour plots showing the

intensity of the displacement field at the substrate's boundary, resulting from the interaction between the displacement amount induced by the adhering cell when optimally arranged and the one imposed by the normal perturbation (depicted as a red point if upward and as a blue one if downward). These results have been obtained by combining the values of ν, P and η mentioned above with the following ones: D = 200 nN, E = 50 kPa and l_D = 60 μm.

consequence, the spontaneous direction in which the cell laid before the application of external perturbations (that, according to the substrate isotropy, should be here random) has no influence. As an example, it is envisaged that if a work quota related to drag forces was taken into account, the multiplicity of optimal configurations would disappear or, at least, would be reduced and the minimum energy solution would be conditioned by the original placement of the cell.

4.2. Cells encircled by a palisade of alternate point loads

When an even number n of orthogonal perturbations is applied, it is possible to envisage patterns such that downward-pointing loads alternate with upward-pointing ones at the vertexes of the corresponding polygonal fence on the substrate's surface, their resultant being, in this way, overall zero.

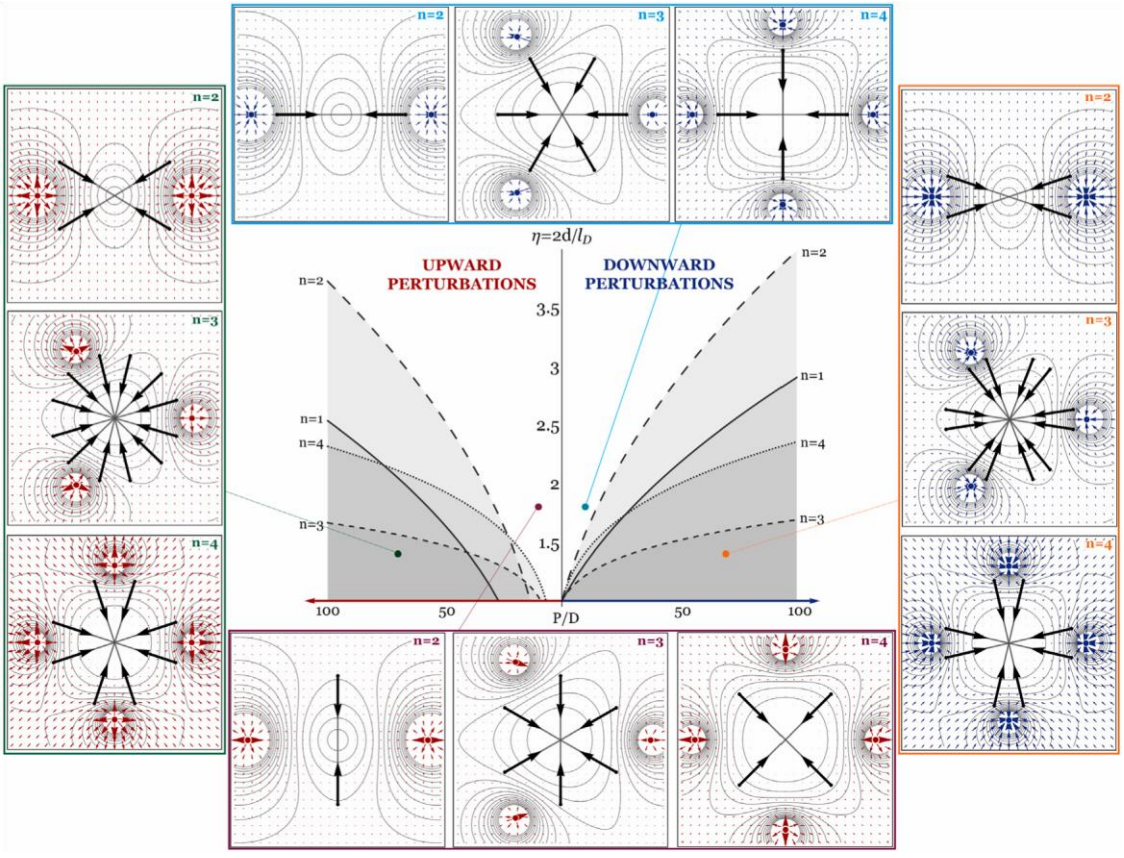

Fig. 3. At the centre, a plot illustrating, for both upward- and downward-pointing perturbations, the partition of the plane P/D–η (where each point identifies the properties of the n applied perturbations in terms of magnitude and distance from the dipole centre) into domains (grey-coloured), defined by the limitations in Eq. (4.4), within which cell's optimal orientations are provided by solution in (4.3), and complementary regions where the configurations associated to the minimum deformation work are given by (4.5). The characteristic size of such domains depends, in addition to the direction of the point loads, on the substrate Poisson ratio – here $\nu = 1/3$ – and on the specific number of perturbations — here $n = 1,2,3,4$. At the four sides of the figure, there are sketches (top views) of the optimal configurations (multiple in some cases) that a cell-dipole would adopt when adhering on the top of a substrate having $\nu = 1/3$ where a fence of 2, 3 or 4 normal forces was applied. For both the possible directions of the perturbations, two pairs of parameters P/D–η have been selected, that are $P/D = 70$ with $\eta = 1.4$ (green and orange points) and $P/D = 10$ with $\eta = 1.8$ (magenta and cyan points), in order to show all the circumstances under which the cell can be found for each considered n. In the sketches, the cell is depicted as a couple of converging black arrows, while on the background there are the level curves (grey solid lines) and the vector plot (red and blue arrows respectively for upward and downward perturbations) describing the displacement induced by the normal perturbations (represented as red points if upward and as blue ones if downward). The side plots have been obtained by also assuming $D = 200$ nN, $E = 50$ kPa and $l_D = 60$ μm.

In such a case, by employing again the superposition principle, the displacement fields provided by the Boussinesq's solution (A.5) specialized for each perturbing force can be combined and used into Eq. (3.5), thus obtaining a null interaction energy if $n/2$ is an odd number, while the following expression when $n/2$ is even too:

$$W_{int.} = \frac{2PD(1+\nu)(1-2\nu)\eta^{n/2}(1-\eta^n)n\cos(n\theta/2)}{\pi E l_D \left[1+\eta^2-2\eta^n\cos(n\theta)\right]} \qquad (4.6)$$

Then, by adding the interaction energy contribution to the cell's self-energy given in Eq.≡ (3.9), one finds two significantly different results depending on whether n is a multiple of 4 or not. In the latter event, since W_{int} 0 and W_D does not depend on the specific orientation, the cell has no possibility to exploit the presence of the strain field induced by the external fence of applied forces for reducing the work that it performs in deforming the substrate. As a consequence, it could orient indifferently along any line passing through its centre. On the contrary, in the complementary situation, that is when n is multiple of 4, limited configurations could be helpfully adopted by the cell in order to reach an optimal state. In particular, by using the energies expressions in (3.9) and (4.6), one obtains that optimal dipole's orientations are represented by the solutions of Eq. (3.10), namely:

$$\tilde{\theta} = \pm_2 \left(\left\{ \arccos\left[\left[(1-\eta^n)(1-2\nu)nP + \sqrt{[(1-\eta^n)(1-2\nu)nP]^2 + [18D(1+\eta^n)]^2} \right] \right] + 2k\pi \right) \right\}, \quad n \left(\left[\frac{}{36D\eta^{n2}} \right] \right) \tag{4.7}$$

$k \in Z,$

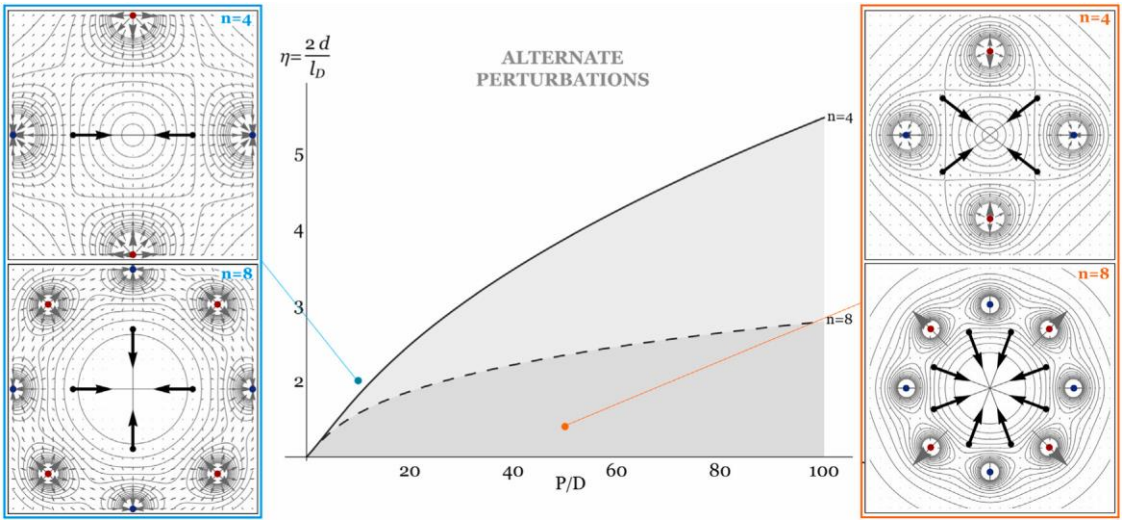

Fig. 4. At the centre, a plot illustrating, in case of perturbations with alternating directions, the partition of the plane P/D–η into domains (grey-coloured), defined by the limitations in Eq. (4.8), within which cell's optimal orientations are provided by solution in (4.7), and complementary regions where minimum deformation work configurations are reached through solution (4.9). The characteristic size of such domains depends on the substrate Poisson ratio – here $\nu = 1/3$ – and on the specific number of perturbations — here $n = 4{,}8$. At the lateral sides of the figure, there are sketches (top views) of the optimal configurations (multiple in some cases) that a cell-dipole would adopt under the influence of 4 and 8 alternate perturbations when $\nu = 1/3$, $E = 50$ kPa, $D = 200$ nN and $l_D = 60$ μm, for a case in which $P/D = 50$ with $\eta = 1.4$ (orange point) and a case of $P/D = 10$ with $\eta = 2$ (cyan point), in order to fall respectively into and outside the domains described by (4.8). In the sketches, the cell is depicted as a couple of converging black arrows, while on the background there are the level curves (grey solid lines) and the vector plot (grey arrows) illustrating the displacement induced by the alternate normal perturbations (represented as red points when upward and as blue ones when downward).

under the following conditions concerning the perturbating forces:

$$1\eta \leq \eta^a := \left[\left[\left[\left[(1-2\nu)nP + \sqrt{[(91-2\nu)nP]^2 + 81D^2} \right] \right] \right]^{2/n}, \quad \forall P, \tag{4.8}$$

$|$

D

while, outside such domain, placements of minimum work magnitude are given by the solutions of Eq. (3.11), here reading as:

$$\tilde{\theta} = \frac{4}{n}k\pi, k \in \mathrm{Z}. \tag{4.9}$$

Therefore, as well as for concordant perturbations, also for alternate ones (with even $\leq \leq n2$), the P/D–η space can be divided into domains such that $1\ \eta\ \eta_a$ (as an example, see grey-coloured regions in Fig. 4, obtained for $\nu = 1/3$ and $n = 4{,}8$), whose points identify perturbations with properties allowing the cell to reach the most favourable condition $W = 0$, and outside which, on the contrary, the cell can minimize but not nullify the work spent through the deformation of the substrate.

It is worth highlighting, also for the current problem, the dependence of the solution on the material and forces parameters ν, η and P/D within the above-mentioned regions and non-involvement of such parameters outside them, where, however, the sole loads' number n weights.

4.3. Remarks on the cell's pursuit of the maximum elongation

It was highlighted above that, in case of concordant and alternate pointing directions of the exogenous normal loads, the cell's optimal orientations are attained at the null points of $|W|$ if inequalities (4.4) and (4.8) hold true and at the stationary conditions (4.5) and (4.9) if the same inequalities are instead violated.

Additionally, Eqs. (4.4) and (4.8) can be used to define, as a function of the substrate's Poisson ratio and of the exogenousto-endogenous forces' magnitudes ratio, when the prescribed loads can be considered at *large distance* from the cell-dipole, that is the distance beyond which the cell can only minimize, but never nullify, the function $|W|$ by orienting in a way that depends on the sole number of external forces. Some results concerning this situation are illustrated in Fig. 5, where polygonal distributions of normal loads acting at large distance from the cell centre are considered.

According to what observed in presence of a single perturbation with reference to the bottom lateral sketches in Fig. 2, it is found that, for any n, the cell-dipole attains its minimum energy configurations by minimizing the distance of its axis from the points of application of downward loads and by maximizing the distance from the vertexes in which upward forces act. Such behaviour can be also explained by the fact that these orientations allow the cell to undergo the highest extension with respect to all the other diametrical fibres of the circumference containing the cell's sites of adhesion, as evidenced in Fig. 5.

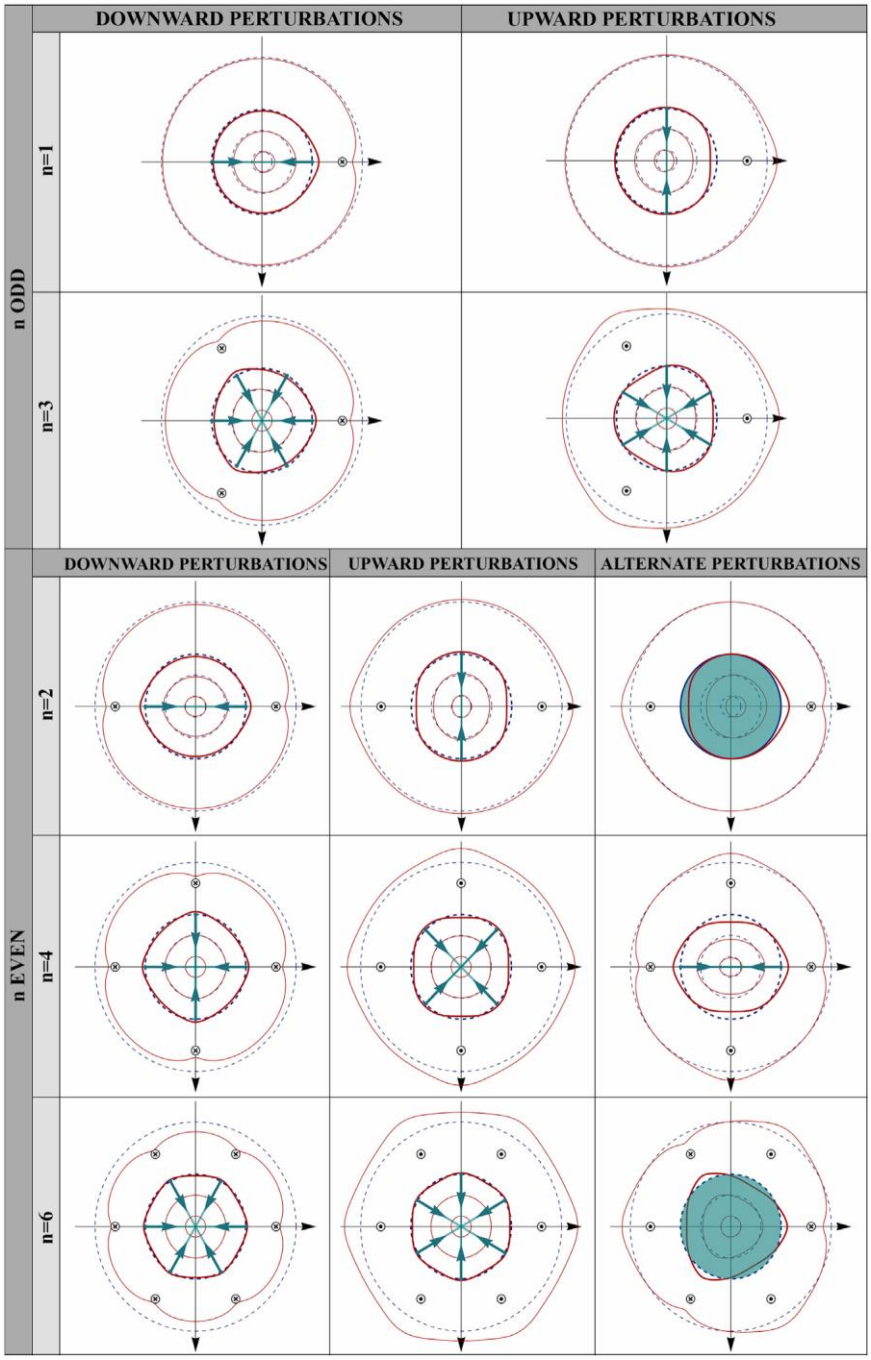

Fig. 5. Synoptic table illustrating the cell-dipole's optimal configurations given by the stationary points in Eqs. (4.5) and (4.9), for concordant and alternate directions respectively, under the action of normal perturbations fences whose parameters P and η are such to fall outside the domains described by Eqs. (4.4) and (4.8). Here, the following values of the parameters have been setted: $\nu = 1/3$, $E = 50$ kPa, $\ell_D = 60$ μm, $D = 200$ nN, $\eta = 1.6$ and $P = 5D$. In the upper part of the table the sole possible cases of all downward-pointing and all upward-pointing loads are shown for odd numbers of applied perturbations ($n = 1,3$), while in the bottom part also the case of alternate loads

directions is considered for even numbers of perturbations (n = 2,4,6). Top views of the dipoles are sketched through pairs of cyan converging arrows, while full cyan-coloured circles are used when there is no preferential orientation. Normal forces acting on the substrate are indicated with a cross when downward and with a circle when upward. Finally, there are shown the deformations undergone by the substrate points lying on the circumference to which the extremities of the dipole belong and on some concentric ones, due to the effect of the external perturbations. Dashed blue lines indicate circumferences in undeformed states while solid red lines their deformed configurations. To the aim of making the deformation detectable, an amplification of the displacement equal to 50 has been used.

The reason why the optimal orientations given by the stationary points of $|\mathcal{W}|$ coincide with the directions of maximum stretch starting from the reference state of a cell acting alone on the substrate, is the following. From the expressions (4.2) and (4.6) of the interaction work spent by the dipole due to the presence of external forces, respectively with concordant and alternate pointing

]]

directions, one can find that there exists at least an angle $\theta \in -\pi/2,\pi/2$ such that $\mathcal{W}_{int} = 0$. This means that, by exploring the whole range, such energy assumes necessarily both positive and negative values and hence, when added to the positive and constant aliquot $\mathcal{W}_D$, it provides a total amount either crossing zero values (as when conditions (4.4) and (4.8) are verified) or, as in the $|\mathcal{W}| \equiv \mathcal{W}$ by verifying Eq. (3.11), due to the independence of $\mathcal{W}_D$ from θ, match the minima of the sole interaction energy, whose case here considered, remaining positive for any θ. In this latter case, the stationary points (4.5) and (4.9), that thus minimize

corresponding values are necessarily negative for what illustrated above. This means – according to Eq. (3.5) – that the change of length induced on the cell at such optimal orientations occurs in the direction opposite to that of the dipole forces and thus produces the maximum extension.

These results are in agreement with previous findings revealing that cell-dipoles tend to align along the direction of uniaxial stretches when prescribed statically to the substrate and to form cells strings over elastic media (Bischofs and Schwarz, 2003; Bischofs et al., 2004). In such cases, indeed, the hypothesis of large distance from the cell can be considered as implicitly assumed, since the cell is modelled as point-like rather than a finite size dipole. Also, the axis of application of the exogenous stresses and that of alignment of neighbouring cells represent the directions of maximum elongation, along which each cell can attain the minimum interaction energy with the environment to reduce the work spent while deforming the elastic substrate.

On this ground, the cells' pursuit of the direction of maximum elongation through the minimization of the sole interaction energy due to external loads, which is generally read as the cells' preference for the highest effective stiffness (Bischofs and Schwarz, 2003), can be interpreted as a special case of the more general optimal condition requiring the minimization – at the best, the cancellation – of the magnitude of whole work that the cell does to deform the

substrate. This, in turn, results into a minimization – again, at the best, the cancellation – of the overall deformation felt by the cell as a consequence of the combination of its own traction forces and of the exogenous loads applied to the half-space.

Finally, a duplex effect can be observed for cases of orthogonal perturbations applied in alternate directions, which can be considered when n is an even number. In this situation the overall resultant load is null but there exist forces configurations that in fact do not have any effect on the dipole orientation – i.e. when $n/2$ is odd – and others such that the cell can however detect the presence of the perturbations and take advantage from it — namely when $n/2$ is even too. In the former event, as Fig. 5 shows for $n = 2,6$, there arise pairs of normal loads pointing towards opposite directions and placed symmetrically with respect to the dipole centre, whose action is not detectable by the cell since the coupled downward and upward forces mutually balance and annihilate their effects: in this way, the dipole does not undergo changes of length – and the interaction energy is null – for any orientation θ. On the other hand, in the complementary case, as illustrated in Fig. 5 for $n = 4$, the symmetric allocation of the external loads fence provides the formation of pairs of concordant loads at diametrically opposite vertexes that reciprocally reinforce their effects, thus interfering constructively rather then destructively and in this manner allowing the cell to sense and exploit their action by selecting the most convenient orientations in terms of elastic work.

5. Cell mechanotropism guided by fences of tangent forces

Complementarily to the case of normal forces, in this Section we analyse the mechanotropism of an adherent cell by assuming that a regular fence of n point loads acts tangentially on the substrate's surface, surrounding the cell-dipole. The ith exogenous force can be hence written by specializing $\mathbf{P}_i$ in Eq. (3.3) for $P_i = P$, $\phi_i = \pi/2$, $d_i = d = \eta l_D/2$ ($\eta > 1$) and $\alpha_i = (i-1)2\pi/n$, $\forall i \in \{1,\dots,n\}$, so that:

$$\mathbf{P}_i = P\cos\gamma_i\hat{\mathbf{e}}_x + \sin\gamma_i\hat{\mathbf{e}}_y,\ \mathbf{x}_{Pi} = d\left\{\cos\left[(i-1)\frac{2\pi}{n}\right]\mathbf{e}_x + \sin\left[(i-1)\frac{2\pi}{n}\right]\mathbf{e}_y\right\}, \tag{5.1}$$

the value of γ_i depending on the orientation of the load.

By employing the expressions of the displacement fields related to this kind of perturbations via the Cerruti's solution (A.8) for calculating the interaction energy (3.5), one can derive the analytical form of the problems (3.10) and (3.11) that would provide the cell optimal orientations for the case at hand. However, differently from the condition involving normal forces, no closed-form solutions can be obtained and numerical procedures were therefore employed to get the results shown in what follows. In particular, the most representative outcomes emerged in the cases of centrifugal forces (i.e. directed outward with respect to the centre of the dipole and associated to $\gamma_i = \alpha_i$) and twisting forces (i.e. $\gamma_i = \alpha_i - \pi/2$). They are illustrated in Figs. 6 and 7,

where different number, position and magnitude of exogenous point loads as well as substrate elasticity are considered.[1]

As in the case of normal loads, the results show how cell-dipoles align along directions such to either nullify the work magnitude $|\mathcal{W}|$ or minimize it at stationary angles by following different paths as a function of the combination of the governing parameters. By way of example, Figs. 6 and 7 show that the optimal configurations associated to forces at growing distances significantly change with both the number of the point loads and their magnitude. In particular, cell-dipoles reorient very differently as the loads are

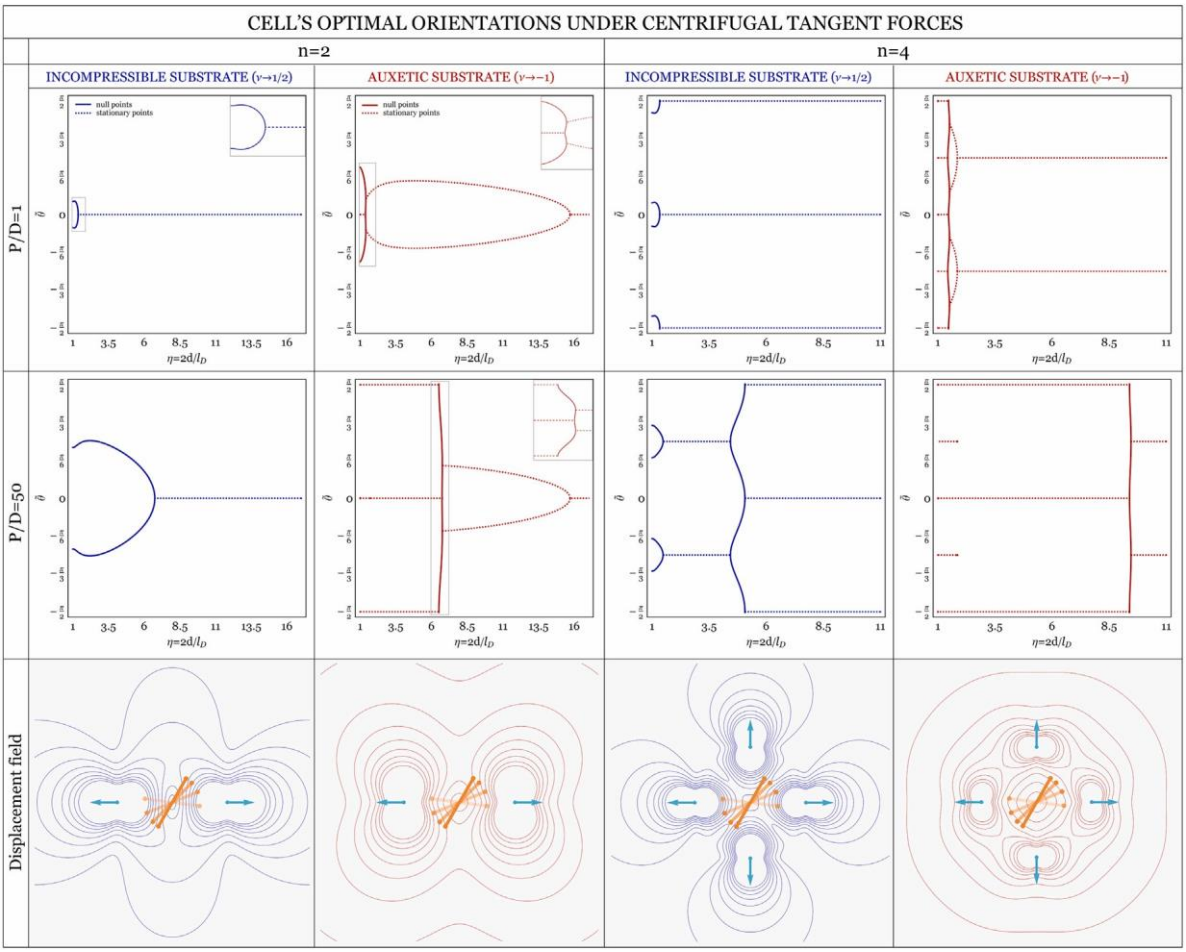

Fig. 6. Optimal orientations predicted for the cell-dipole as an effect of the interaction with palisades of centrifugal tangent forces, which induce on the substrate's surface a displacement field exemplified at the bottom of the figure. Without loss of generality, results are shown in function of the relative distance $\eta = 2d/l_D$ for $n = 2$ and $n = 4$ point loads and exogenous-to-endogenous forces' magnitude ratios $P/D = 1,50$, by making reference to substrate's Poisson ratios

[1] Note that the domains of validity of the results obtained for the cases of point forces acting tangentially to the substrate's boundary, should be evaluated on the basis of the set of prescribed model's parameters, according to what reported in the Appendix for the Cerruti's singular solution. This means that, in general, a lower bound should be considered for the relative distance η, in a way that the dipole's adhesion sites are part of such domains. However, one can verify that, in the cases shown in Figs. 6 and 7, the outcomes are admissible for any $\eta > 1$, the region of incompatibility of the Cerruti's solution vanishing for $\nu \to 1/2$ as well as for $\nu \to -1$.

ν approaching the incompressibility limit ($\nu \to 1/2$) and the extremely auxetic value ($\nu \to -1$). Herein, solid tracts represent angles nullifying the elastic work $|\mathcal{W}|$ while dotted ones identify its stationary (minimum) points.

comparable to cell's tractions ($P/D = 1$) and as the forces' ratio becomes high ($P/D = 50$), the influence of this parameter however vanishing at large distances.

Additionally, despite the case of orthogonal loads had already highlighted the dominant role played by the Poisson ratio in cells' mechanotropism, the presence of tangent forces revealed some new and unprecedented effects on the dipole optimal orientation, the cells exhibiting a very different behaviour, accompanied by configurational switches, if the substrate material is assumed to be auxetic.

As an example, the application at large distance of $n = 4$ centrifugal point loads leads to have polarizations that depend strongly on whether cells are sitting on standard media (i.e. with positive Poisson ratio) or they adhere on highly auxetic materials (i.e. with negative Poisson ratio). In fact, one finds that, in the first case, cells orient along the directions of the external forces ($\tilde{\vartheta} = 0, \pm\pi/2$), in the latter condition instead deviating with respect to the axes of the point loads of $\pm\pi/4$. However, this result varies with the number of applied tangent forces and, for instance, is lost at large distance if $n = 2$, when, independently from ν, the dipole reaches the configuration of minimum work at $\tilde{\vartheta} = 0$, similarly to the case in which uniaxial deformation regimes are imposed to the substrate (Collinsworth et al., 2000; Bischofs and Schwarz, 2003; Xu et al., 2018; Chen et al., 2013; Steward et al., 2009; Liu et al., 2013). Analogous considerations can be inferred for the twisting distributions of point loads.

Overall, Figs. 6 and 7 also highlight how the relative distance η plays the role of a bifurcation parameter. Indeed, as critical values of η are achieved, the cell switches from null work points to different kinds of stationary states and conversely, the auxeticity of the substrate further significantly enriching the landscape of achievable configurations. In this regard, it is finally worth to note that, unlike the case of applied normal forces, for tangent loads we can no longer recognize mutually exclusive regions (defined in terms of the model's parameters) in which either angular or stationary points of $|\mathcal{W}|$ provide minima. In fact, optimal configurations

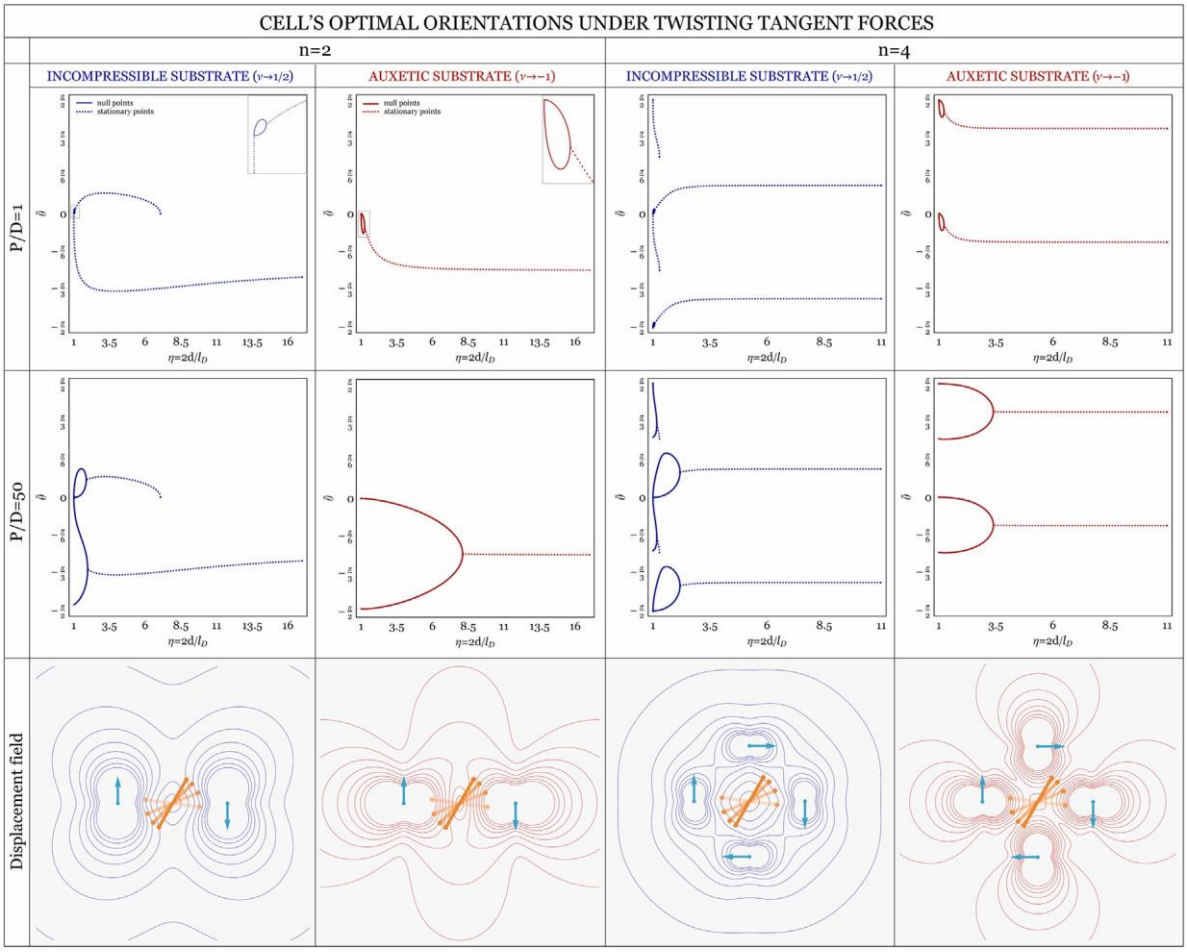

Fig. 7. Optimal orientations minimizing the magnitude of work spent by the cell-dipole to deform the substrate when surrounded by tangent point forces determining a twisting effect on the substrate's surface, which is associated to a displacement field exemplified at the bottom of the figure. Without loss of generality, results are shown in function of the relative distance $\eta = 2d/l_D$ for $n = 2$ and $n = 4$ point loads and for exogenous-to-endogenous forces' magnitude ratios $P/D = 1,50$, by making reference to substrate's Poisson ratios ν approaching the incompressibility limit ($\nu \to 1/2$) and the extremely auxetic value ($\nu \to -1$). Herein, solid tracts represent angles nullifying the elastic work $|W|$ while dotted ones identify its stationary (minimum) points.

associated to both null work and work's stationary points may co-exist in some cases and multiple solutions at different elastic work's levels and related to local minima could be found as well. While multiplicity of the solutions is a mathematical result and it is expected that in real conditions cells could prefer only one among these optimal orientations, the model would help to explain why cells would polarize along selected directions, attracted by energetically convenient configurations that are closest to their unperturbed states.

6. Conclusions and perspectives

The present work investigates the mechano-induced reorientation – here named *mechanotropism* – of an elongated cell, adhering to an elastic substrate and encircled by a *palisade* of exogenous point loads.

By using Cerruti's solutions, the fibre-like stationary (i.e. non-migrating) cell has been modelled as a dipole of contractile forces transmitted to the underlying elastic medium at two separate focal adhesion points, thereby generalizing previous approaches describing simply the cell as a point force dipole. Indeed, the latter treatments are valid only if the distance between the external loads and the single-cell is much larger than the size of the cell, a condition difficult to be achieved in many experiments, where instead a finite cell-force distance is required to take into account realistic length scales.

Combined Boussinesq's and Cerruti's solutions have been then employed to model the action of regular polygonal patterns of normal and tangent point loads applied to the substrate and surrounding the cell-dipole.

On this basis, by formulating a minimization problem involving as objective function the magnitude of work done by the cell to deform the substrate stressed by cell's tractions and exogenous loads, multiple optimal cell orientations have been found. It has been highlighted that, depending on the substrate Poisson ratio and on the number, direction, distance from the cell and magnitude of the applied forces, two different minimization criteria for seeking optimal configurations can be followed in parallel. In the first, the cell exploits the strain field induced by the neighbouring forces for nullifying the work spent against the substrate deformation by aligning along selected preferential directions. In the second case, no orientation does exist such that the cell can reach the ideal status of zero work of deformation, the sole chance being to minimize its value by positioning at optimal angles.

Analytical and numerical model outcomes have revealed that the Poisson ratio is the sole relevant mechanical property for the cell mechanotropism when force-prescribed boundary conditions are considered, in such a case the stiffness being not involved to decide the optimal polarization — a result somehow complementary with respect to that of durotaxis, where stiffness (gradient) drives the cell locomotion. From the mechanical point of view, this complementarity could be physically explained by considering that, while in mechano- or duro-taxis the cell moves *translating* on the surface and in this way senses – and is somehow driven by – substrate *inhomogeneities* induced by stress or stiffness gradients, in mechanotropism the cell polarizes *rotating* on the same surface, so seeking for the best configuration by exploring the substrate properties directly related to what is responsible for deformation *anisotropies*, that is the Poisson ratio in case of isotropic materials. Furthermore, the study of the influence of exogenous tangent forces on the alignment of the cell-dipole have led to never highlighted configurational switches when considering auxetic materials. These findings could hence help to shed light on the role played by the Poisson ratio of the elastic environment (e.g. extra-cellular matrix or engineered scaffolds) in mechanotransduction processes that have been recently demonstrated to influence the growth and differentiation of adherent cells (Yan et al., 2017; Zhang et al., 2013).

Despite improvements have to be introduced to enrich the model by considering mechanical nonlinearities, as well as the work spent by cells to rotate, to polymerize/depolymerize actin filaments and to dismantle/re-build focal adhesion sites, the quite simple feasibility of the proposed approach traces back several experimental observations and shows how some non-trivial cells' configurations can be recovered with the sole weapons of elasticity. In fact, the results suggest that, at least in principle, it would be possible to probe the physical rules driving the orientation of single-cells adhering to deformable substrates by means of the application of *ad hoc* designed patterns of normal and tangent (or even inclined) forces, by modulating few key parameters.

It is felt that the present work could also contribute to better understand some still unclear mechanisms of cell polarization involved in important processes such as wound healing, tissues morphogenesis and remodelling, in turn suggesting possible unexplored applications of interest for translational and precise medicine. By exploiting the interplay between cell's orientation and selected polygonal fences of prescribed point loads, one might in fact apply the method for several purposes, for instance to indirectly measure via atomic force microscopy (AFM) endogeneous forces and stresses in the cell actin fibres, to induce duplication or differentiation by favouring or enforcing homeostatic cells' stretches, as well as to envisage new mechanics-based markers for targeting cancer cells or for guessing pathological conditions from cells' mechanotropism.

Declaration of competing interest

The authors declare that they have no known competing financial interests or personal relationships that could have appeared to influence the work reported in this paper.

Acknowledgements

The Authors desire to acknowledge the anonymous Reviewer for his/her observations and suggestions, which contributed to improve the quality of the present work. SP, AC, LD, NP and MF then acknowledge the support of the Italian Ministry of Education, University and Research (MIUR) through the grant ''Integrated mechanobiology approaches for a precise medicine in cancer treatment'' (grant number: PRIN-20177TTP3S). MF, LD and NP also acknowledge the support of the MIUR, Italy through the grant ''Micromechanics and robotics for diagnosis and therapy in prostate cancer'' (grant number: PON-ARS01_01384). LD and NP are also supported by the European Commission H2020 FET Proactive ''Neurofibres'' grant (grant number: 732344) as well as by the MIUR, Italy under the ''Departments of Excellence'' grant (grant number: L.232/2016). NP also acknowledges the support of the FET Open ''Boheme'' grant (grant number: 863179). ARC acknowledges the support of the grant ''Programma Operativo Nazionale Ricerca e Innovazione 2014-2020 - AIM: Attraction and International Mobility'' (grant number: PON-AIM1849854-1).

Appendix. Summary of the Boussinesq's and Cerruti's solutions

By considering an elastostatic displacement formulation that accounts for Saint-Venant compatibility conditions and constitutive assumptions of homogeneous and isotropic materials,

equilibrium equations governing linear elasticity theory result in the following Navier–Cauchy equation (Landau and Lifshitz, 1970):

$$\mu\nabla^2\mathbf{u} + (\lambda + \mu)\nabla\nabla\cdot\mathbf{u} + \mathbf{B} = \mathbf{0}, \tag{A.1}$$

where $\mathbf{u}$ is the unknown displacement vector field to be determined by obeying the prescribed (Dirichlet- or Neumann-type) boundary conditions associated to the system of partial differential equations, $\mathbf{B}$ is the body force vector field, $\mu = E/[2(1 + \nu)]$ and $\lambda = 2\mu\nu/(1-2\nu)$ are the Lamè constants of the continuum body, E being its Young modulus and ν the Poisson ratio, while $\nabla^2(\cdot)$, $\nabla(\cdot)$ and $\nabla\cdot(\cdot)$ denote the Laplacian, gradient and divergence operators, respectively.

In the second half of the 1880s, Betti provided a first general method for the integration of such a system (Love, 1982), founded on his reciprocal work theorem (Timoshenko and Goodier, 1967). On these bases, Cerruti and Boussinesq subsequently developed solutions for the equilibrium problem in the particular case of point forces acting – tangentially and normally, respectively – on the plane boundary of an isotropic elastic half-space (Love, 1982). Then, different derivations of such solutions have been given over the time (Timoshenko and Goodier, 1967; Johnson, 1985; Barber, 1992), in particular Westergaard formulating an interpretation in terms of Galerkin vector (Westergaard, 1952). In a general case, such vector allows to express the solution of the basic equations of linear elasticity (A.1) in the form:

$$2\mu\mathbf{u} = 2(1-\nu)\nabla[\nabla^2\boldsymbol{\Gamma} - \nabla\nabla\cdot\boldsymbol{\Gamma}], \tag{A.2}$$

where $\boldsymbol{\Gamma}$ is the Galerkin vector, that – by substitution into (A.1) – has to satisfy the equation:

$$\nabla^4\boldsymbol{\Gamma} = -\frac{\mathbf{B}}{1-\nu}, \tag{A.3}$$

this meaning that, in case of negligible body forces, it has to be a biharmonic vector function.

Specifically, by fixing a Cartesian reference system $\geq \{x,y,z\}$ and by considering a point load acting normally to the boundary of a semi-infinite solid occupying the half-space $z \geq 0$, under null body forces ($\mathbf{B} = \mathbf{0}$), the Boussinesq's problem can be solved – by virtue of the superposition principle holding true in linear frameworks – through additive combination of the following Galerkin vectors $\boldsymbol{\Gamma}^{B}$ and $\boldsymbol{\Gamma}^{B}$, in a way that shear stresses vanish on the plane boundary $z = 0$ (Westergaard, 1952):

$$\boldsymbol{\Gamma}^{B}{}_1 = 2F\pi^{z}\rho\hat{\mathbf{e}}_z,\ \boldsymbol{\Gamma}^{B}{}_2 \text{ s.t. } \nabla\cdot\boldsymbol{\Gamma}^{B}{}_2 = \left(1 - 2_{2\pi\nu}\right)F^{z}\log(\rho + Z),\ \nabla^2\boldsymbol{\Gamma}_2{}^{B} = \mathbf{0}, \tag{A.4}$$

where $X := x - x_F$, $Y := y - y_F$ and $Z := z$, hence $\rho := \sqrt{X^2 + Y^2 + Z^2}$ is the distance of the generic point of the half-space, say $\mathbf{x} = x\hat{\mathbf{e}}_x + y\hat{\mathbf{e}}_y + z\hat{\mathbf{e}}_z$, from the point of application of the external force, namely $\mathbf{x}_F = x_F\hat{\mathbf{e}}_x + y_F\hat{\mathbf{e}}_y$, while $\hat{\mathbf{e}}_j$, with $j = x,y,z$, is the generic unit vector of the selected

rectangular reference system and F_z is the sole non-vanishing component of the normal point load $\mathbf{F}_B = F_z\hat{\mathbf{e}}_z$ acting at $\mathbf{x}_F$. We recall that the harmonic scalar function $-\nabla\cdot\boldsymbol{\Gamma}_2^B$ is also known as strain potential and may be in general used, independently from the definition of Galerkin vector, for describing some purely irrotational deformation fields (Barber, 1992). By then assuming $\boldsymbol{\Gamma} = \boldsymbol{\Gamma}^B + \boldsymbol{\Gamma}^B$ in Eq. (A.2), the displacement field that solves Boussinesq's problem is given

1 2

by $\mathbf{u}_B$ having the following scalar components:

$$u_x^B = \frac{F_z}{4\pi\mu\rho_3}\left[XZ - (1-2\nu)\frac{X}{\rho(\rho+Z)}\right], \tag{A.5a}$$

$$u_y^B = \frac{F_z}{4\pi\mu\rho_3}\left[YZ - (1-2\nu)\frac{Y}{\rho(\rho+Z)}\right], \tag{A.5b}$$

$$u_z^B = \frac{F_z}{4\pi\mu\rho_3}\left[Z^2 + 2(1-\nu)\right]. \tag{A.5c}$$

On the other hand, Cerruti's problem – that concerns the complementary case of semi-infinite solid interesting the half-space $z \geq 0$ undergoing a purely tangent point load at $z = 0$, for negligible body forces – is solved by the superposition of the Galerkin vector

$$\frac{1}{4\pi(1-\nu)}\left[(F_x\hat{\mathbf{e}}_x + F_y\hat{\mathbf{e}}_y) + (1-2\nu)\log(\rho+Z)(F_xX + F_yY)\hat{\mathbf{e}}_z\right] \tag{A.6}$$

$\boldsymbol{\Gamma} = \rho F_x\mathbf{e}$

with the strain potential

$$-\nabla\cdot\boldsymbol{\Gamma}_2^C = \frac{(1-2\nu)}{2\pi(\rho+Z)}(F_xX + F_yY), \quad {}^2\boldsymbol{\Gamma}_2^C = \nabla\mathbf{0}, \tag{A.7}$$

herein F_x and F_y being the non-null components of the tangent point load $\mathbf{F}_C = F_x\hat{\mathbf{e}}_x + F_y\hat{\mathbf{e}}_y$ acting at $\mathbf{x}_F$ (Westergaard, 1952). As a consequence, analogously to the Boussinesq's previous problem, by substituting $\boldsymbol{\Gamma} = \boldsymbol{\Gamma}^C + \boldsymbol{\Gamma}^C$ into Eq. (A.2), the Cerruti's solution,

1 2 guaranteeing null

normal stress over the boundary, is given by the displacement field $\mathbf{u}_C$ whose components read as:

$$u_x^C = \frac{1}{4\pi\mu}\left\{\left[\rho\rho_2 - (\rho+Z)2F_y + \rho + \rho_3 + (1-2\nu)F_x\right]\left[\frac{1}{\rho+Z} - \frac{X^2}{\rho(\rho+Z)^2}\right]\right\}, \tag{A.8a}$$

$$u_y = \frac{1}{4\pi\mu}\left\{\left[\frac{XY}{\rho\rho^2} - \frac{1}{1-2\nu}\left(\frac{1}{\rho+Z}\right)^2 F_x + \left[\frac{1}{\rho} + \frac{Y^2}{\rho^3} + (1-2\nu)\frac{1}{\rho+Z} - \frac{Y^2}{(\rho+Z)^2}\right]F_y\right\}, \quad \text{(A.8b)}$$

$$u_z = \frac{1}{4\pi\mu}\left[\frac{Z}{\rho^3} + (1-2\nu)\left(\frac{X}{\rho(\rho+Z)}F_x + \frac{Y}{\rho(\rho+Z)}F_y\right)\right]. \quad \text{(A.8c)}$$

Finally, by virtue of the linearity, the mechanical response of an elastic half-space in general undergoing combinations of normal and/or tangent point loads can be obtained by employing the superposition principle (Timoshenko and Goodier, 1967) to couple displacements solutions of the types (A.5) and (A.8). In particular, superposed Boussinesq's and Cerruti's solutions are used in the present work with the aim to explore optimal orientations attained by a single-cell adhering to the flat boundary of a linear elastic substrate under the perturbing effects of externally applied point loads.

Validity domains of singular solutions. It is worth recalling that, when fundamental solutions are adopted, due to their singularity at the point of application of the load (i.e. divergence of the resulting displacements, strains and stresses), there exist regions of the half-space where the local injectivity (or equivalently the orientation-preserving condition) given by the strict positiveness of the determinant of the deformation gradient tensor, is violated, that means:

$$J := \det(\mathbf{I} + \nabla\mathbf{u}) \simeq 1 + \nabla\cdot\mathbf{u} \leq 0. \quad \text{(A.9)}$$

In particular, when dealing with the Boussinesq's solution (A.5) for a point load acting normally to the half-space surface, one can found that

$$J_B := 1 + \nabla\cdot\mathbf{u}_B > 0 \Leftrightarrow \frac{F_z Z}{\rho^3} < \frac{2\pi\mu}{1-2\nu},$$

( )

a condition everywhere verified on the boundary $Z = z = 0$ since $\lim_{Z\to 0} F_z Z/\rho^3 = 0 \;\forall\; \{X,Y\} \neq 0$ and the right side of the
inequality is strictly positive for any admissible Poisson ratio.

On the other hand, with regard to the Cerruti's problem, the spatial domain in which the solution provided in Eq. (A.8) turns out to be inconsistent can be identified as follows

$$J_C := 1 + \nabla\cdot\mathbf{u}_C \leq 0 \Leftrightarrow \frac{F_x X + F_y Y}{\rho^3} \geq \frac{2\pi\mu}{1-2\nu}\rho. \quad \text{(A.10)}$$

application of the tangent force $\mathbf{F}_C$ – which contains the planar domain $J_C|_{z=0} \leq 0$ is given by: It can be shown that the radius of the smallest circular region – lying on the half-space boundary $z = 0$ and centred at the point of

$$r_C = \frac{c}{4}(1-2\nu). \quad \text{(A.11)}$$

$$|\mathbf{F}$$

$$2\pi\mu$$

This quantity assumes its maximum value when $\nu = -1/4$ and, in such case, its variability depends on the sole ratio between the≥ magnitude of the applied force and the stiffness of the medium occupying the half-space $z\,0$, i.e.:

$$r_C|_{\nu=-1/4} = 2\sqrt{32} \quad \frac{}{\pi} \quad |\mathbf{F}_C| \,. \tag{A.12}$$

Then, with reference to the case of the cell-dipole, by considering average values found in literature (Prager-Khoutorsky et al., 2011; Ghibaudo et al., 2008; Schwarz et al., 2002; Balaban et al., 2001; Style et al., 2014), it is possible to estimate an upper limit for this radius, say r^{max}_C, by substituting into Eq. (A.12) an upper bound value for $|\mathbf{F}_C|$ (i.e. $|\mathbf{F}_C| = 1\mu N$) and a lower one for E (i.e. $E = 10$ kPa). Therefore, for a cell (e.g. a fibroblast) exhibiting a length $l_D \approx 50\text{-}60$ μm, one can estimate $r^{max}_C \approx l_D/10$. On this basis, the compatibility of the displacement field due to each cell traction force is guaranteed for points of the substrate boundary at a distance al least equal to r^{max}_C from the focal adhesion site.

References

Balaban, N.Q., Schwarz, U.S., Riveline, D., Goichberg, P., Tzur, G., Sabanay, I., Mahalu, D., Safran, S., Bershadsky, A., Addadi, L., Geiger, B., 2001. Force and focal adhesion assembly: A close relationship studied using elastic micropatterned substrates. Nature Cell Biol. 3 (5), 466–472.

Banerjee, S., Gardel, M.L., Schwarz, U.S., 2020. The actin cytoskeleton as an active adaptive material. Annu. Rev. Condens. Matter Phys. 11 (1), 421–439.

Bao, G., Suresh, S., 2003. Cell and molecular mechanics of biological materials. Nature Mater. 2 (11), 715.

Barber, J.R., 1992. Elasticity. Springer Netherlands.

Ben-Yaakov, D., Golkov, R., Shokef, Y., Safran, S.A., 2015. Response of adherent cells to mechanical perturbations of the surrounding matrix. Soft Matter 11 (7), 1412–1424.

Bershadsky, A.D., Balaban, N.Q., Geiger, B., 2003. Adhesion-dependent cell mechanosensitivity. Annu. Rev. Cell Dev. Biol. 19 (1), 677–695.

Bischofs, I.B., Safran, S.A., Schwarz, U.S., 2004. Elastic interactions of active cells with soft materials. Phys. Rev. E 69 (2).

Bischofs, I.B., Schwarz, U.S., 2003. Cell organization in soft media due to active mechanosensing. Proc. Natl. Acad. Sci. 100 (16), 9274–9279.

Bischofs, I.B., Schwarz, U.S., 2005. Effect of Poisson ratio on cellular structure formation. Phys. Rev. Lett. 95 (6).

Brand, C.A., Linke, M., Weißenbruch, K., Richter, B., Bastmeyer, M., Schwarz, U.S., 2017. Tension and elasticity contribute to fibroblast cell shape in three dimensions. Biophys. J. 113 (4), 770–774.

Carotenuto, A.R., Cutolo, A., Palumbo, S., Fraldi, M., 2019. Growth and remodeling in highly stressed solid tumors. Meccanica 54 (13), 1941–1957.

Carotenuto, A., Cutolo, A., Petrillo, A., Fusco, R., Arra, C., Sansone, M., Larobina, D., Cardoso, L., Fraldi, M., 2018. Growth and in vivo stresses traced through tumor mechanics enriched with predator-prey cells dynamics. J. Mech. Behav. Biomed. Mater. 86, 55–70.

Chen, B., Chen, X., Gao, H., 2015a. Dynamics of cellular reorientation on a substrate under biaxial cyclic stretches. Nano Lett. 15 (8), 5525–5529.

Chen, B., Ji, B., Gao, H., 2015b. Modeling active mechanosensing in cell–matrix interactions. Annu. Rev. Biophys. 44 (1), 1–32.

Chen, B., Kemkemer, R., Deibler, M., Spatz, J., Gao, H., 2012. Cyclic stretch induces cell reorientation on substrates by destabilizing catch bonds in focal adhesions. In: Pelling, A. (Ed.), PLoS ONE 7 (11), e48346.

Chen, Y., Pasapera, A.M., Koretsky, A.P., Waterman, C.M., 2013. Orientation-specific responses to sustained uniaxial stretching in focal adhesion growth and turnover. Proc. Natl. Acad. Sci. 110 (26), E2352–E2361.

Cohen, O., Safran, S.A., 2016. Elastic interactions synchronize beating in cardiomyocytes. Soft Matter 12, 6088–6095.

Collinsworth, A.M., Torgan, C.E., Nagda, S.N., Rajalingam, R.J., Kraus, W.E., Truskey, G.A., 2000. Orientation and length of mammalian skeletal myocytes in response to a unidirectional stretch. Cell Tissue Res. 302 (2), 243–251.

De, R., Zemel, A., Safran, S.A., 2007. Dynamics of cell orientation. Nat. Phys. 3 (9), 655–659.

De, R., Zemel, A., Safran, S.A., 2008. Do cells sense stress or strain? Measurement of cellular orientation can provide a clue. Biophys. J. 94 (5), L29–L31.

Deguchi, S., Ohashi, T., Sato, M., 2006. Tensile properties of single stress fibers isolated from cultured vascular smooth muscle cells. J. Biomech. 39 (14), 2603–2610.

Deibler, M., Spatz, J.P., Kemkemer, R., 2011. Actin fusion proteins alter the dynamics of mechanically induced cytoskeleton rearrangement. In: Kreplak, L. (Ed.), PLoS ONE 6 (8), e22941.

Dembo, M., Wang, Y.-L., 1999. Stresses at the cell-to-substrate interface during locomotion of fibroblasts. Biophys. J. 76 (4), 2307–2316.

Discher, D.E., Janmey, P., Wang, Y.-l., 2005. Tissue cells feel and respond to the stiffness of their substrate. Science 310 (5751), 1139–1143.

Eastwood, M., Mudera, V., McGrouther, D., Brown, R., 1998. Effect of precise mechanical loading on fibroblast populated collagen lattices: morphological changes. Cell Motil. Cytoskeleton 40 (1), 13–21.

Engler, A.J., Sen, S., Sweeney, H.L., Discher, D.E., 2006. Matrix elasticity directs stem cell lineage specification. Cell 126 (4), 677–689.

Ferreira, J.P.S., Kuang, M., Marques, M., Parente, M.P.L., Damaser, M.S., Natal Jorge, R.M., 2020. On the mechanical response of the actomyosin cortex during cell indentations. Biomech. Model. Mechanobiol. 19 (6), 2061–2079.
Fraldi, M., Carotenuto, A.R., 2018. Cells competition in tumor growth poroelasticity. J. Mech. Phys. Solids 112, 345–367.
Fraldi, M., Palumbo, S., Carotenuto, A., Cutolo, A., Deseri, L., Pugno, N., 2019. Buckling soft tensegrities: Fickle elasticity and configurational switching in living cells. J. Mech. Phys. Solids 124, 299–324.
Fraldi, M., Palumbo, S., Carotenuto, A., Cutolo, A., Pugno, N., 2021. Generalized multiple peeling theory uploading hyperelasticity and pre-stress. Extreme Mech. Lett. 42, 101085.
Friedrich, B.M., Safran, S.A., 2012. How cells feel their substrate: spontaneous symmetry breaking of active surface stresses. Soft Matter 8, 3223–3230.
Fusco, S., Panzetta, V., Netti, P.A., 2017. Mechanosensing of substrate stiffness regulates focal adhesions dynamics in cell. Meccanica 52 (14), 3389–3398.
Geiger, B., Bershadsky, A., Pankov, R., Yamada, K.M., 2001. Transmembrane crosstalk between the extracellular matrix and the cytoskeleton. Nature Rev. Mol. Cell Biol. 2 (11), 793–805.
Geiger, B., Spatz, J.P., Bershadsky, A.D., 2009. Environmental sensing through focal adhesions. Nature Rev. Mol. Cell Biol. 10 (1), 21–33.
Ghibaudo, M., Saez, A., Trichet, L., Xayaphoummine, A., Browaeys, J., Silberzan, P., Buguin, A., Ladoux, B., 2008. Traction forces and rigidity sensing regulate cell functions. Soft Matter 4.
Goli-Malekabadi, Z., Tafazzoli-Shadpour, M., Rabbani, M., Janmaleki, M., 2011. Effect of uniaxial stretch on morphology and cytoskeleton of human mesenchymal stem cells: static vs. dynamic loading. Biomed. Tech./Biomed. Eng. 56 (5), 259–265.
Golkov, R., Shokef, Y., 2017. Shape regulation generates elastic interaction between living cells. New J. Phys. 19 (6), 063011.
Harris, A.K., Stopak, D., Wild, P., 1981. Fibroblast traction as a mechanism for collagen morphogenesis. Nature 290 (5803), 249–251.
Harris, A., Wild, P., Stopak, D., 1980. Silicone rubber substrata: a new wrinkle in the study of cell locomotion. Science 208 (4440), 177–179.
Hayakawa, K., Sato, N., Obinata, T., 2001. Dynamic reorientation of cultured cells and stress fibers under mechanical stress from periodic stretching. Exp. Cell Res. 268 (1), 104–114.
He, S., Green, Y., Saeidi, N., Li, X., Fredberg, J.J., Ji, B., Pismen, L.M., 2020. A theoretical model of collective cell polarization and alignment. J. Mech. Phys. Solids 137, 103860.
He, S., Su, Y., Ji, B., Gao, H., 2014. Some basic questions on mechanosensing in cell–substrate interaction. J. Mech. Phys. Solids 70, 116–135.
Hsu, H.-J., Lee, C.-F., Kaunas, R., 2009. A dynamic stochastic model of frequency-dependent stress fiber alignment induced by cyclic stretch. PLoS One 4 (3), e4853.
Ingber, D.E., Wang, N., Stamenović, D., 2014. Tensegrity, cellular biophysics, and the mechanics of living systems. Rep. Progr. Phys. 77 (4), 046603.
Iskratsch, T., Wolfenson, H., Sheetz, M.P., 2014. Appreciating force and shape—the rise of mechanotransduction in cell biology. Nature Rev. Mol. Cell Biol. 15

(12), 825.
Johnson, K.L., 1985. Contact Mechanics. Cambridge University Press.
Jungbauer, S., Gao, H., Spatz, J.P., Kemkemer, R., 2008. Two characteristic regimes in frequency-dependent dynamic reorientation of fibroblasts on cyclically stretched substrates. Biophys. J. 95 (7), 3470–3478.
Kaunas, R., Hsu, H.-J., 2009. A kinematic model of stretch-induced stress fiber turnover and reorientation. J. Theoret. Biol. 257 (2), 320–330.
Kong, D., Ji, B., Dai, L., 2008. Stability of adhesion clusters and cell reorientation under lateral cyclic tension. Biophys. J. 95 (8), 4034–4044.
Kopfer, K.H., Jäger, W., Matthäus, F., 2020. A mechanochemical model for rho GTPase mediated cell polarization. J. Theoret. Biol. 504, 110386. Lakes, R., 1987. Foam structures with a negative Poisson's ratio. Science 235 (4792), 1038–1040.
Landau, L.D., Lifshitz, E., 1970. Theory of Elasticity, Vol. 7. Pergamon,
Lazopoulos, K.A., Stamenović, D., 2008. Durotaxis as an elastic stability phenomenon. J. Biomech. 41 (6), 1289–1294.
Lim, J.Y., Donahue, H.J., 2007. Cell sensing and response to micro- and nanostructured surfaces produced by chemical and topographic patterning. Tissue Eng. 13 (8), 1879–1891.
Lin, F., Du, F., Huang, J., Chau, A., Zhou, Y., Duan, H., Wang, J., Xiong, C., 2016. Substrate effect modulates adhesion and proliferation of fibroblast on graphene layer. Colloids Surfaces B 146, 785–793.
Liu, C., Baek, S., Kim, J., Vasko, E., Pyne, R., Chan, C., 2013. Effect of static pre-stretch induced surface anisotropy on orientation of mesenchymal stem cells. Cell. Mol. Bioeng. 7 (1), 106–121.
Livne, A., Bouchbinder, E., Geiger, B., 2014. Cell reorientation under cyclic stretching. Nature Commun. 5.
Lo, C.-M., Wang, H.-B., Dembo, M., li Wang, Y., 2000. Cell movement is guided by the rigidity of the substrate. Biophys. J. 79 (1), 144–152.
Loewe, B., Serafin, F., Shankar, S., Bowick, M.J., Marchetti, M.C., 2020. Shape and size changes of adherent elastic epithelia. Soft Matter 16, 5282–5293.
Love, A.E.H., 1982. A Treatise on the Mathematical Theory of Elasticity. Cambridge university press.
Maul, T.M., Chew, D.W., Nieponice, A., Vorp, D.A., 2011. Mechanical stimuli differentially control stem cell behavior: morphology, proliferation, and differentiation. Biomech. Model. Mechanobiol. 10 (6), 939–953.
Mofrad, M.R.K., Kamm, R.D. (Eds.), 2009. Cellular Mechanotransduction. Cambridge University Press (CUP).
Nelson, C.M., Jean, R.P., Tan, J.L., Liu, W.F., Sniadecki, N.J., Spector, A.A., Chen, C.S., 2005. Emergent patterns of growth controlled by multicellular form and mechanics. Proc. Natl. Acad. Sci. 102 (33), 11594–11599.
Pelham, R.J., Wang, Y.l., 1997. Cell locomotion and focal adhesions are regulated by substrate flexibility. Proc. Natl. Acad. Sci. 94 (25), 13661–13665.

Plotnikov, S.V., Sabass, B., Schwarz, U.S., Waterman, C.M., 2014. High-resolution traction force microscopy. In: Methods in Cell Biology. Elsevier, pp. 367–394.

Prager-Khoutorsky, M., Lichtenstein, A., Krishnan, R., Rajendran, K., Mayo, A., Kam, Z., Geiger, B., Bershadsky, A.D., 2011. Fibroblast polarization is a matrix-rigidity-dependent process controlled by focal adhesion mechanosensing. Nature Cell Biol. 13 (12), 1457–1465.

Riveline, D., Zamir, E., Balaban, N.Q., Schwarz, U.S., Ishizaki, T., Narumiya, S., Kam, Z., Geiger, B., Bershadsky, A.D., 2001. Focal contacts as mechanosensors:
externally applied local mechanical force induces growth of focal contacts by an mdia1-dependent and ROCK-independent mechanism. J. Cell Biol. 153 (6), 1175–1186.

Sabass, B., Gardel, M.L., Waterman, C.M., Schwarz, U.S., 2008. High resolution traction force microscopy based on experimental and computational advances. Biophys. J. 94 (1), 207–220.

Schwarz, U., Balaban, N., Riveline, D., Bershadsky, A., Geiger, B., Safran, S., 2002. Calculation of forces at focal adhesions from elastic substrate data: The effect of localized force and the need for regularization. Biophys. J. 83 (3), 1380–1394. Schwarz, U.S., Safran, S.A., 2002. Elastic interactions of cells. Phys. Rev. Lett. 88 (4).

Schwarz, U.S., Safran, S.A., 2013. Physics of adherent cells. Rev. Modern Phys. 85 (3), 1327–1381.

Stamenović, D., Ingber, D.E., 2009. Tensegrity-guided self assembly: from molecules to living cells. Soft Matter 5 (6), 1137–1145.

Steward, R.L., Cheng, C.-M., Wang, D.L., LeDuc, P.R., 2009. Probing cell structure responses through a shear and stretching mechanical stimulation technique. Cell Biochem. Biophys. 56 (2–3), 115–124.

Style, R.W., Boltyanskiy, R., German, G.K., Hyland, C., MacMinn, C.W., Mertz, A.F., Wilen, L.A., Xu, Y., Dufresne, E.R., 2014. Traction force microscopy in physics and biology. Soft Matter 10, 4047–4055.

Tamiello, C., Buskermolen, A.B.C., Baaijens, F.P.T., Broers, J.L.V., Bouten, C.V.C., 2015. Heading in the right direction: Understanding cellular orientation responses to complex biophysical environments. Cell. Mol. Bioeng. 9 (1), 12–37.

Tan, J.L., Tien, J., Pirone, D.M., Gray, D.S., Bhadriraju, K., Chen, C.S., 2003. Cells lying on a bed of microneedles: An approach to isolate mechanical force. Proc. Natl. Acad. Sci. 100 (4), 1484–1489.

Timoshenko, S., Goodier, J., 1967. Theory of Elasticity 3rd ed., 1970. p. 142,

Tondon, A., Kaunas, R., 2014. The direction of stretch-induced cell and stress fiber orientation depends on collagen matrix stress. In: Kumar, S. (Ed.), PLoS ONE 9 (2), e89592.

Wang, J.H.-C., Goldschmidt-Clermont, P., Wille, J., Yin, F.C.-P., 2001. Specificity of endothelial cell reorientation in response to cyclic mechanical stretching. J. Biomech. 34 (12), 1563–1572.

Wang, H., Ip, W., Boissy, R., Grood, E.S., 1995. Cell orientation response to cyclically deformed substrates: Experimental validation of a cell model. J. Biomech. 28 (12), 1543–1552.

Wang, N., Tytell, J.D., Ingber, D.E., 2009. Mechanotransduction at a distance: mechanically coupling the extracellular matrix with the nucleus. Nature Rev. Mol. Cell Biol. 10 (1), 75–82.

Wei, Z., Deshpande, V.S., McMeeking, R.M., Evans, A.G., 2008. Analysis and interpretation of stress fiber organization in cells subject to cyclic stretch. J. Biomech. Eng. 130 (3), 031009.

Westergaard, H.M., 1952. Theory of Elasticity and Plasticity. Harvard University Press.
Xu, G.-K., Feng, X.-Q., Gao, H., 2018. Orientations of cells on compliant substrates under biaxial stretches: A theoretical study. Biophys. J. 114 (3), 701–710.
Yan, Y., Li, Y., Song, L., Zeng, C., 2017. Pluripotent stem cell expansion and neural differentiation in 3-D scaffolds of tunable Poisson's ratio. Acta Biomaterialia 49, 192–203.
Zhang, W., Soman, P., Meggs, K., Qu, X., Chen, S., 2013. Tuning the Poisson's ratio of biomaterials for investigating cellular response. Adv. Funct. Mater. 23 (25), 3226–3232.